The Cuban staircase sequences of coral reef and marine terraces: A forgotten masterpiece of the Caribbean geodynamical puzzle

Article *in* Marine Geology · July 2021

DOI: 10.1016/j.margeo.2021.106575

Kevin Pedoja
Université de Caen Normandie

Christine Authemayou
Université de Bretagne Occidentale

Arelis Nuñez
Instituto de Geología y Paleontología; Cuba

Denovan Chauveau
Université de Bretagne Occidentale

Marine Geology 440 (2021) 106575

Contents lists available at ScienceDirect

Marine Geology

journal homepage: www.elsevier.com/locate/margo

The Cuban staircase sequences of coral reef and marine terraces: A forgotten masterpiece of the Caribbean geodynamical puzzle

Leandro Peñalver [a], Kevin Pedoja [b,*], Denyse Martin-Izquierdo [a], Christine Authemayou [c], Arelis Nuñez [a], Denovan Chauveau [c], Gino de Gelder [e], Pedro Davilan [d], Laurent Husson [e]

[a] *Institute of Geology and Paleontology, La Habana, Cuba*
[b] *Normandie Univ, Unicaen, Unirouen, CNRS, M2C, 14 000 Caen, France*
[c] *LGO, IUEM, CNRS, UMR 6538, Université de Bretagne Occidental, UBO, Plouzané, France*
[d] *Univ Moa, Moa, Cuba*
[e] *Univ. Grenoble Alpes, CNRS, ISTerre, Grenoble, France*

ARTICLE INFO

Editor: Prof Edward Anthony

Keywords:
Glacial cycle
Pleistocene
Caribbean
Cuba
Marine and coral reef terraces

ABSTRACT

The emerged sequences of coral reef and marine terraces of the Cuban Archipelago have been recognized since the end of the 19th century but with noticeable exceptions, their bio-constructions and/or deposits are not dated. The northern Caribbean islands and associated archipelagos are located in a left-lateral strike-slip tectonic setting, at the boundary between the North America and Caribbean plates. Cuba is the only landmass located on the American Plate directly adjacent to this transform fault zone. Quantifying upper Pleistocene coastal uplift is thus key to elucidate the recent vertical deformation of the Caribbean geodynamic puzzle with regards to the active tectonic segmentation of this area. We compiled bibliographic data and present new measurements concerning the Cuban sequences of coral reef and marine terraces; maximum elevations, minimum number of successive strandlines and elevation of the lowermost terrace. The Cuban Archipelago exhibits five main uplifting coastal stretches separated by subsiding areas, with at least 23 emerged staircase sequences of coastal terraces. At four sites, the lowest coral reef terrace has been previously correlated to the Last Interglacial Maximum (MIS 5e, 122 ± 6 ka). At nine sites, we extended the morpho-stratigraphy to derive Upper Pleistocene apparent and eustasy-corrected uplift rates. Alongshore Cuba, MIS 5e coastal terraces and associated shoreline angles occur at elevations ranging from 7 m to 40 m, yielding eustasy-corrected uplift rates ranging from 0.06 ± 0.01 mm.yr^{-1} (NW Cuba) to 0.33 ± 0.01 mm.yr^{-1} (SE Cuba). More than 400 km northward of the transform fault, eustasy-corrected uplift rates (0.13 mm.yr^{-1}) suggest that the whole Cuban Archipelago is affected by the North America/Caribbean plate motion, with a partitioned compressive component resulting in block tectonics with tilting controlled by regional faults.

1. Introduction

Sequences of marine and coral reef terraces, herein called coastal terraces, are widespread indicators of Late Cenozoic coastal tectonics and sea levels (e.g. Lyell, 1830; Darwin, 1842; Davis, 1915; Daly, 1925; Berry et al., 1966; Broecker et al., 1968; Montaggioni and Braithwaite, 2009; Pedoja et al., 2011, 2014; Murray-Wallace and Woodroffe, 2014; Hibbert et al., 2016). Within the Caribbean Sea, islands and archipelagos exhibit emerged sequences of coastal terraces. Most studied are the coastal landforms correlated to Marine Isotopic Stage 5e (MIS 5e, 122 ± 6 ka); for instance in the West Indies (Feuillet et al., 2004; Léticée et al., 2019), in Curacao, Bonaire, Aruba (Alexander, 1961; Hippolyte and Mann, 2011) and in Jamaica (e.g. Horsfield, 1975; Szabo, 1979; Mitchell et al., 2000, 2001). The island of Barbados displays one of the most studied sequence of coral reef and marine terraces (Mesolella, 1967; Broecker et al., 1968; James et al., 1971; Schellmann and Radtke, 2004; Schellmann et al., 2004) which constitutes a benchmark for sea level and climate studies over the last 1 Ma (Murray-Wallace and Woodroffe, 2014). The Late Cenozoic sequences of coastal terraces of the two largest Caribbean islands and archipelagos, Cuba and Hispaniola, have been recognized since a long time (Crosby, 1883; Darwin, 1890; Agassiz, 1894; Spencer, 1895), and considered as an “ensemble” together with

* Corresponding author.
E-mail address: kevin.pedoja@unicaen.fr (K. Pedoja).

https://doi.org/10.1016/j.margeo.2021.106575
Received 20 April 2021; Received in revised form 22 July 2021; Accepted 23 July 2021
Available online 31 July 2021

Barbados, Jamaica (Jones, 1918; Trechmann, 1933) and the Cayman Islands (Matley, 1926; Brunt et al., 1973; Emery, 1981; Woodroffe et al., 1983; Spencer, 1985; Coyne et al., 2007). The formation of such sequences is related to vertical deformation associated with the *Great Antillean/Northern Caribbean* fault zone (Taber, 1922; Woodring, 1954), at the boundary between the North American and Caribbean plates. Recent studies including absolute dating are rather scarce, for example for Haiti (Dumas et al., 2006; Hearty et al., 2007), for the Dominican Republic (Diaz de Neira et al., 2015, 2017; Escuder-Viruete et al., 2020), and for Cuba (Toscano et al., 1999; Pajon et al., 2006; De Waele et al., 2017, 2018; Muhs et al., 2018; Schielein et al., 2020).

For the Cuban Archipelago, descriptions of the coastal landforms are abundant and contain quantified geomorphic data (e.g. Vaughan and Spencer, 1902; Meinzer, 1933; Massip, 1936; Marie-Victorin and Léon, 1956; Ducloz, 1963; Iturralde-Vinent, 1967, 1969a, 1969b, 1977, 1981, 1982, 1994, 2003; Kartashov and Mayo, 1974; Kartashov and Mayo, 1976; Kartashov et al., 1981; Shantzer et al., 1976; Peñalver, 1982; Peñalver et al., 1982a, 1982b, 1997; Peñalver et al., 1998; Franco, 1983; Pushcharovski, 1988; Salomon, 1995; Cabrera and Peñalver, 2001; Perez-Aragon et al., 2001). Combining field observations with a synthesis of previous literature, we describe the distribution of the Cuban staircase sequences of coastal terraces and propose quantitative morphometrics, such as their maximum elevations and the minimum number of successive terraces. Studies including U/Th (Toscano et al., 1999; Pajon et al., 2006; De Waele et al., 2017, 2018; Muhs et al., 2018), ESR (Schielein et al., 2020) or paleomagnetic dating (Pérez Lazo, 1986; Peñalver et al., 2003), all correlated the lowermost terrace (T1) to the Last Interglacial Maximum (MIS 5e; 122 +/− 6 ka). In the following, we assume this morpho-stratigraphy (T1 = MIS 5e) is correct for sequences of coastal landforms including a single terrace or for sequences for which we know the elevation of the lowermost terrace, although we specify the cases in which this is directly confirmed by dating. Using five sea-level curves, we derive 15 relative and absolute Upper Pleistocene uplift rates at 13 sites. This approach allows us to discuss the coastal tectonics of the Cuban archipelago located in the vicinity of the left-lateral Transform Fault Zone between the North American and Caribbean plates.

2. Settings

2.1. *Geodynamics, geology, hydrodynamics*

The Caribbean and Central American region contains two subduction zones, the Lesser Antilles Trench to the East and the Central America Trench to the West, connected through a large transform fault zone (Mann and Burke, 1984; Fig. 1). The transform boundary between the Caribbean plate and North American plate is partitioned into two major active *E*-W left lateral strike-slip fault zones (Mann et al., 1991; Calais and Mercier De Lépinay, 1995). These strike-slip fault zones, seismically active, are located North and South of the Cayman Trough (Perrot et al., 1997; Calais et al., 1992). They extend over ~2000 km and are named the Oriente Transform Fault to the North and the Enriquillo-Plantain-Garden Transform Fault to the South (Calais et al., 1998; Prentice et al., 2010; Leroy et al., 2015). To the East, the two fault zones bound the Gonave-Hispanolia microplate (Fig. 1), and accommodate the strike-slip component of the oblique convergence between the Caribbean and North American plates at a rate of 19 mm·a^{-1} (Symithe et al., 2005; Calais et al., 2016; Fig. 1). The Gonave Hispaniola Block is also affected by shortening, both due to the convergence obliquity of the plate boundary associated with the Bahamas platform collision to the North, and due to the Beata ridge indentation to the South (Mann et al., 1990, Calais et al., 2016; Rojas-Agramonte et al., 2005; Corbeau et al., 2019). South of Cuba Island (Figs.1, 2, 3, 4), the Oriente Transform Fault includes various segments with transtensive and transpressive relay zones and parallel offshore thrusts named the Santiago Deformed Belt (Calais and Mercier De Lépinay, 1995; Leroy et al., 2015; Corbeau et al.,

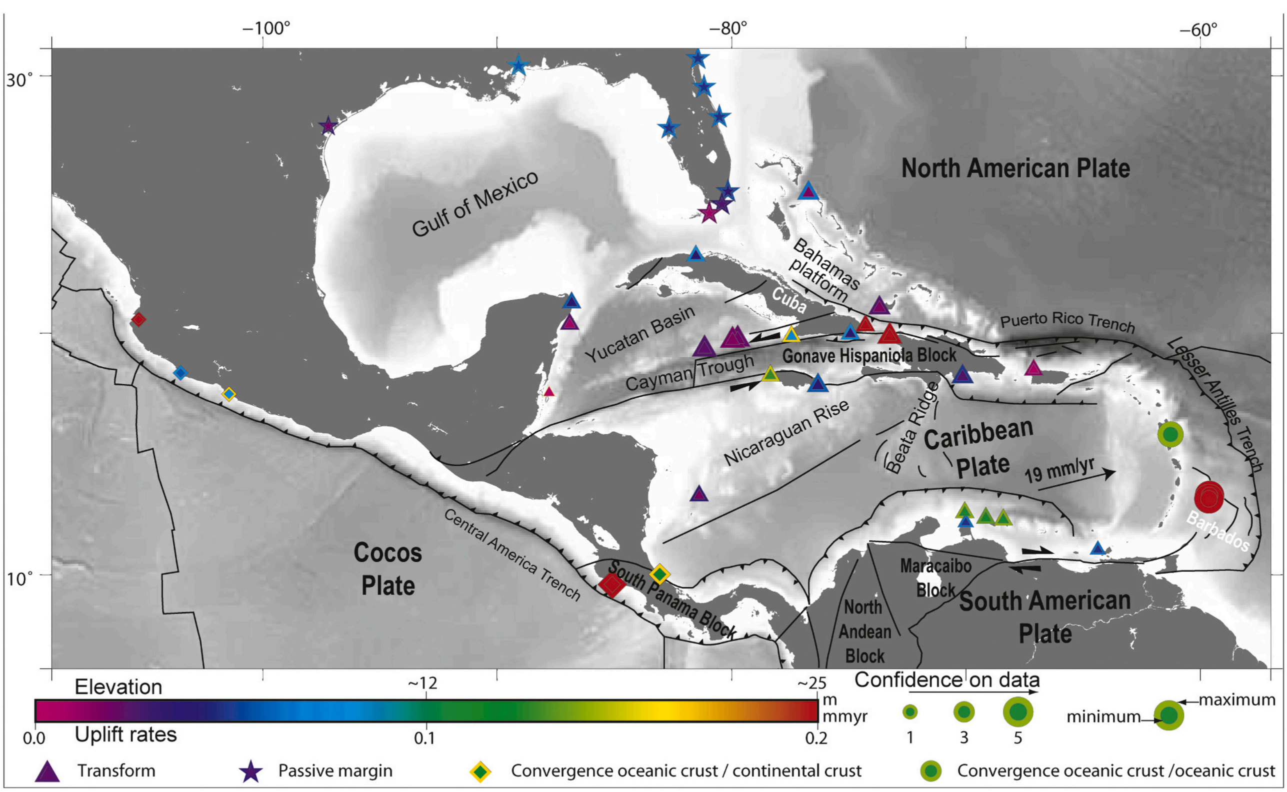

Fig. 1. The Caribbean geodynamical puzzle. MIS 5e data is from Pedoja et al. (2011, 2014), geodynamics and tectonics redrawn from Symithe et al. (2005) and Wessels et al. (2019).

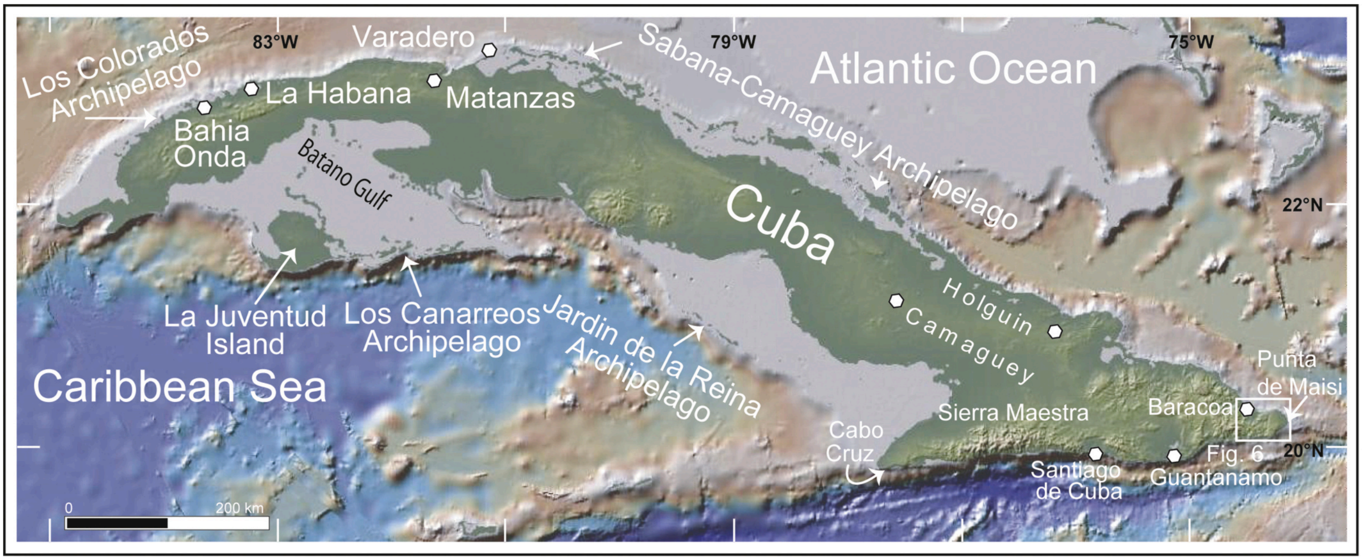

Fig. 2. The Cuban archipelago and toponymy used herein.

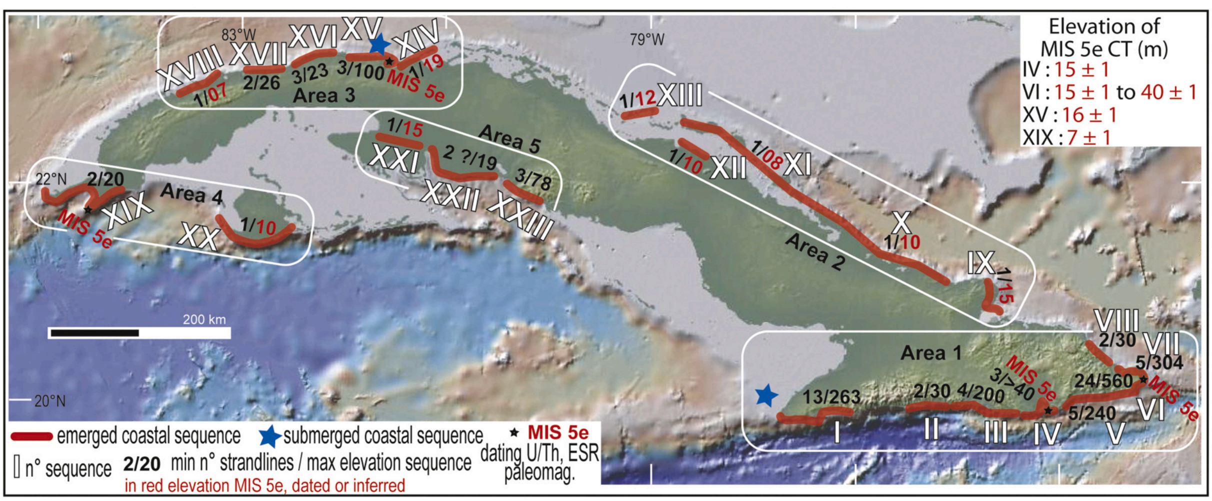

Fig. 3. Distribution of the coastal sequences. Elevations below 30 m have a margin of error of ±1 m, those above ±10 m.

2016; Wessels et al., 2019).

The Cuban archipelago includes a main island and more than 4000 associated islands, islets and *cayos*, all located on a continental platform (Fig. 2). The island belongs to the Great Arc of the Caribbean, which initially formed by subduction along an inter-American Transform Fault at ~135 Ma, during Cretaceous times (Burke, 1988; Pindell et al., 2012; Hastie et al., 2013). During the late Upper Cretaceous, this arc became inactive, collided with the Bahamas carbonate platform and subsequently fragmented to form the Greater Antilles islands (Mann et al., 1995; Cruz-Orosa et al., 2012; Leroy et al., 2000). In Cuba, the Paleocene-Eocene collision between the island arc of the Caribbean plate and Bahamas platform of the North American plate resulted in an ENE-WSW and NW-SE trending orogenic belt (Gordon et al., 1997). This orogenic belt is associated with synorogenic basins and ENE-WSW-trending regional normal and strike-slip faults (Pinar Fault, Trocha Fault, Cauto-Nipe Fault, on Fig. 4) that bound several tectonics blocks and accommodate a part of the westward offshore NW-SE-trending and then NE-SW-trending Yucatan basin opening (Leroy et al., 2000; Pindell et al., 2005; Cruz-Orosa et al., 2012). During the arc/platform collision, the obliquity of the North American/Caribbean plate convergence increased (Gordon et al., 1997; Cruz-Orosa et al., 2012). Since Oligocene time, plate motion is mainly accommodated along the Oriente Transform Fault, South of Cuba Island (Iturralde-Vinent, 1996; Pindell et al., 2005; Rodriguez-Cotilla, 2014; Calais et al., 2016; Alvarez et al., 2017). A vertical motion component along this fault is revealed by pervasive uplifting coastal stretches (Peñalver et al., 2003) and associated sequences of fossil shorelines studied herein (Figs. 2, 3, 4, 5).

The Cuban archipelago is located in a semi-diurnal, micro-tidal area, with tidal ranges from 0.4 to 0. 8 m. Ground swell, mostly coming from the Atlantic Ocean, is consistent only in winter and the wave-height rarely exceeds two meters as the swell is dampened by the Bahamas platform (Colas and Sutherland, 2001). The South part of Cuba Main Island is occasionally subjected to the Antarctic groundswell and affected by hurricanes (Colas and Sutherland, 2001).

2.2. Previous studies of the Cuban coastal terraces

The first mention of the emerged sequences of coastal terraces of

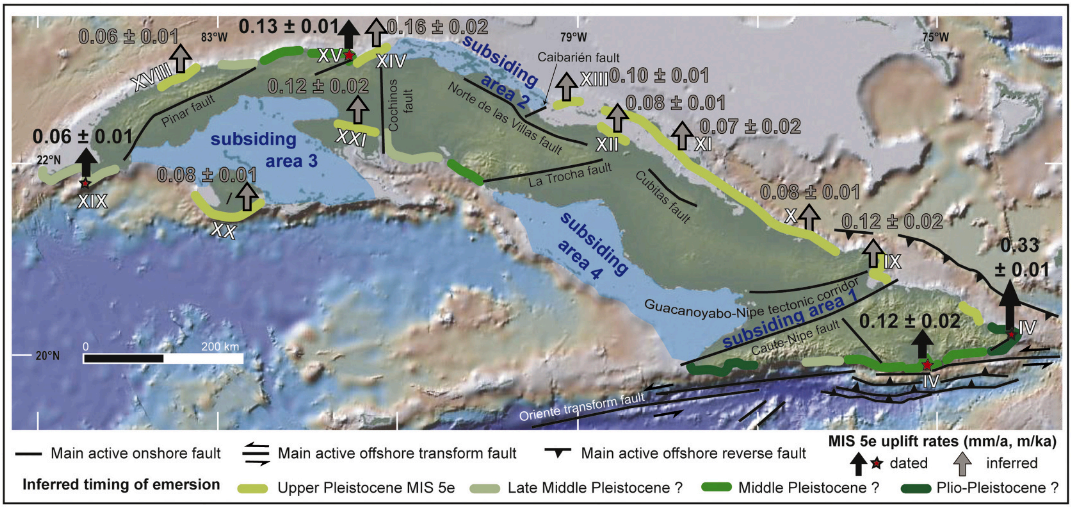

Fig. 4. Coastal uplift and main onshore and offshore faults of the Cuban Archipelago. The possible timing for the emersion of the uplifted coastal stretch of the Cuba Archipelago come from the extrapolation of MIS 5e coastal uplift rates (see text for more details). Tectonics information compiled from Gordon et al., 1997 and Alvarez et al., 2017.

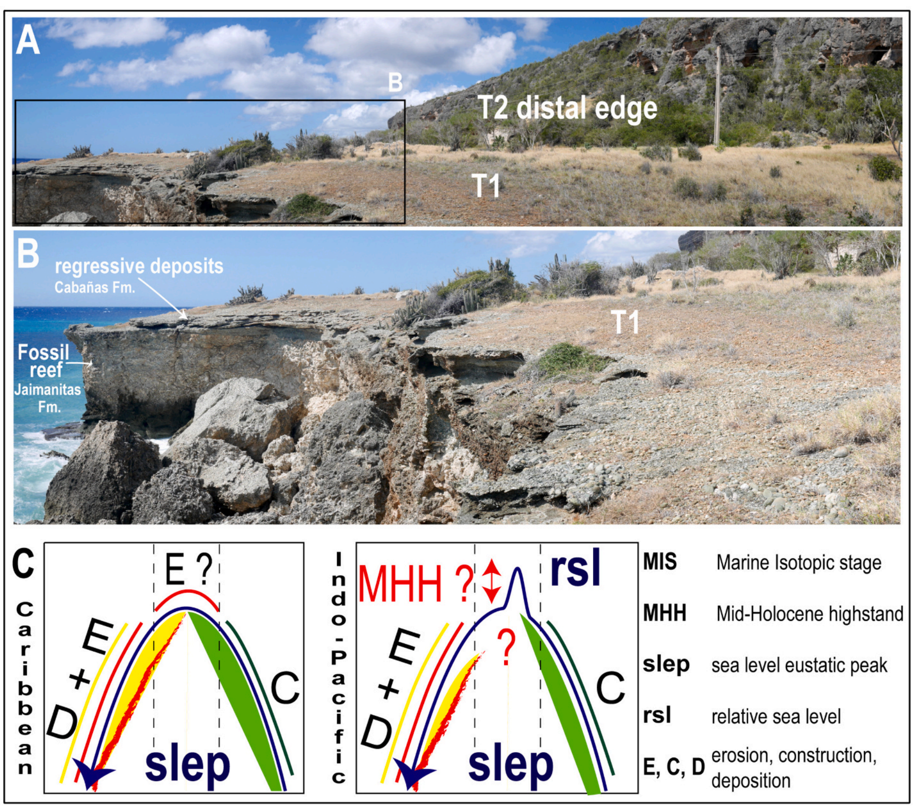

Fig. 5. The lowermost coastal terrace (T1) near Imias A) General view of the composite landform B) Zoom on the distal edge of the coastal terrace. The coastal terrace consist of a reefal limestone unit (Jamainitas Fm.) uncoformably overlain by regressive clastic conglomerates (Cabañas Fm.). C) Comparison of the Indo-Pacific and Caribbean Holocene sea-levels and influence on the processes resulting in coastal terraces formation.

Cuba seems to have been by Crosby (1883), who described emerged fossil reefs near La Habana (NE) and Baracoa (SE; Figs. 2, 3, 4). At the latter site, he described coral limestone up to ~243 m in elevation. By analogy with Jamaica, he proposed that emerged reefs could be present up to ~610 m. Crosby (1883) proposed a 'general' sequence of coastal terraces including four successive reefs with the lowest one found at ~9 m at various sites on the island and the upper one at ~243 m at the mouth of the Rio Yumuri, near Baracoa (Fig. 2; Table 1). Darwin (1890) discussed the possible origin of the South Cuban and Haitian sequences of coastal terraces. Agassiz (1894) sketched some South Cuban sequences. Then Hill (1894, 1895) proposed correlation of some *elevated reefs* across the Island. Spencer (1895) described coastal uplift at Matanzas. Vaughan and Spencer (1902) reported coastal terraces near La Habana - Matanzas, Cabo Cruz, and Punta de Maisi (Table 1). Based on

Table 1
The coastal sequences of the Cuba Archipelago.

Zone	n°	sequence name	Minimum n° level	maximum elevation sequence	Maximum elevation T1	MoE	Dating	Morpho-stratigraphy	Reference
1	I	Cabo Cruz	13	263	–	–	–	–	Crosby, 1883; Agassiz, 1894; Vaughan and Spencer, 1902; Taber, 1931; Massip, 1936; Marie-Victorin and Léon, 1956; Gutiérrez-Domech and Duarte-Barrientos, 2001; Cabrera and Peñalver, 2003; Peñalver et al., 2003; Molerio-Leon, 2005; Cabrera, 2011; Cabrera et al., 2011
1	II	West Santiago	2	30	–	–	–	–	Crosby, 1883; Agassiz, 1894; Vaughan and Spencer, 1902; Taber, 1931; Massip, 1936; Guttierez-Domech and Barrientos-Duarte, 2001; Cabrera and Peñalver, 2003; Cabrera and Peñalver, 2003; Peñalver et al., 2003; Molerio-Leon, 2005; Cabrera, 2011; Cabrera et al., 2011
1	III	East Santiago / Siboney/ San Antonio del Sur	4	200	–	–	–	–	Crosby, 1883; Agassiz, 1894; Vaughan and Spencer, 1902; Vaughan, 1914; Massip, 1936; Guttierez-Domech and Barrientos-Duarte, 2001; Cabrera and Peñalver, 2003; Molerio-Leon, 2005; Cabrera, 2011; Pérez et al., 2011; Cabrera et al., 2011
1	IV	Guantanamo Bay	3	> 40	15	1	15 U/Th dating of corals colonies	T1 = MIS 5e	Taber, 1922; Darton, 1926; Meinzer, 1933; Massip, 1936; Guttierez-Domech and Barrientos-Duarte, 2001; Cabrera and Peñalver, 2003; Molerio-Leon, 2005; Cabrera, 2011; Cabrera et al., 2011; Muhs et al., 2018
1	V	Imias	5	240	–	–	–	–	Crosby, 1883; Agassiz, 1894; Taber, 1922; Meinzer, 1933; Woodring, 1954; Massip, 1936; Guttierez-Domech and Barrientos-Duarte, 2001; Nuñez, 2001; Peñalver et al., 2003; Molerio-Leon, 2005; Cabrera, 2011; Cabrera et al., 2011
1	VI	Maisi	24	560	15 to 40	1	paleomagnetism	T1 = MIS 5e T2 = MIS 7 Summit sequence 3 Ma	Crosby, 1883; Agassiz, 1894; Vaughan and Spencer, 1902; Vaughan, 1914; Taber, 1922; Massip, 1936; del Busto Alvarez, 1975; Pérez Lazo, 1986; Salomon, 1995;Guttierez-Domech and Barrientos-Duarte, 2001; Cabrera and Peñalver, 2003; (Peñalver et al., 2001), Peñalver et al., 2003; Molerio-Leon, 2005; Cabrera, 2011; Cabrera et al., 2011
1	VII	Yumuri	5	304	–	–	–	–	Crosby, 1883; Massip, 1936; Guttierez-Domech and Barrientos-Duarte, 2001; Cabrera and Peñalver, 2003; Molerio-Leon, 2005; Cabrera, 2011; Cabrera et al., 2011
1	VIII	Baracoa	2	30	–	–	–	–	Crosby, 1883; Massip, 1936; Salomon, 1995; Cabrera and Peñalver, 2003; Molerio-Leon, 2005; Dominguez-Gonzalez et al., 2007; Cabrera et al., 2011
2	IX	Banes	1	15	15	1	inferred	T1 = MIS 5e	Guttierez-Domech and Barrientos-Duarte, 2001; Cabrera and Peñalver, 2003; Molerio-Leon, 2005; Cabrera, 2011; Cabrera et al., 2011
2	X	Ciego de Avila SE	1	10	10	1	inferred	T1 = MIS 5e	Guttierez-Domech and Barrientos-Duarte, 2001; Cabrera and Peñalver, 2003; Molerio-Leon, 2005; Cabrera, 2011; Cabrera et al., 2011

(continued on next page)

Table 1 (*continued*)

Zone	n°	sequence name	Minimum n° level	maximum elevation sequence	Maximum elevation T1	MoE	Dating	Morpho-stratigraphy	Reference
2	XI	Ciego de Avila Cayos	1	8	8	1	inferred	T1 = MIS 5e	Guttierez-Domech and Barrientos-Duarte, 2001; Molerio-Leon, 2005; Cabrera et al., 2011
2	XII	Ciego de Avila NE	1	10	10	1	inferred	T1 = MIS 5e	Guttierez-Domech and Barrientos-Duarte, 2001; Cabrera and Peñalver, 2003; Molerio-Leon, 2005; Cabrera, 2011; Cabrera et al., 2011
2	XIII	Cayo Santa Maria	1	12	12	1	inferred	T1 = MIS 5e	Guttierez-Domech and Barrientos-Duarte, 2001; Cabrera and Peñalver, 2003; Molerio-Leon, 2005; Cabrera, 2011; Cabrera et al., 2011
3	XIV	Varadero – Carbonera	1	19	19	1	inferred	T1 = MIS 5e	Massip, 1936; Zenkovichy and Ionin, 1969, Perez-Aragon et al., 2001; Guttierez-Domech and Barrientos-Duarte, 2001; Cabrera and Peñalver, 2003; Molerio-Leon, 2005; Cabrera, 2011; Cabrera et al., 2011
3	XV	Matanzas	3	100	16	1	XX U/Th speleothem in sea-cave and 3 U/Th dating of fossil coral	T1 = MIS 5e	Vaughan and Spencer, 1902; Richards, 1935; Massip, 1936; Zenkovichy and Ionin, 1969; Shakun et al., 2015, Shantzer et al., 1976; Glushankova et al., 1980; Toscano et al., 1999; Budd, 2000; Gutiérrez-Domech and Duarte-Barrientos, 2001; Perez-Aragon et al., 2001; Cabrera and Peñalver, 2003; Pérez et al., 2003; Pérez et al., 2008; Cabrera, 2011; Cabrera et al., 2011; Molerio-Léon, 2017a, 2017b
3	XVI	Santa Cruz del Norte	3	23	–	–	–	–	Zenkovichy and Ionin, 1969; Shanzer et al., 1975, Shantzer et al., 1976; Toscano et al., 1999; Gutiérrez-Domech and Duarte-Barrientos, 2001; Perez-Aragon et al., 2001; Cabrera and Peñalver, 2003; Pérez et al., 2008; Cabrera, 2011; Cabrera et al., 2011
3	XVII	La Habana	2	26	–	–	–	–	Zenkovichy and Ionin, 1969; Shanzer et al., 1975, Shantzer et al., 1976; Naprstek, 1978; Gutiérrez-Domech and Duarte-Barrientos, 2001; Perez-Aragon et al., 2001; Cabrera and Peñalver, 2003; Molerio-Leon, 2005; Perera and Rojas, 2005; Pérez et al., 2008; Cabrera et al., 2011; Rojas et al., 2017
3	XVIII	Mariel- Harlem – Bahia Honda	1	7	7	1	inferred	T1 = MIS 5e	Zenkovich and Ionin, 1969, Perez-Aragon et al., 2001; Molerio-Leon, 2005; Cabrera, 2011; Cabrera et al., 2011
4	XIX	Peninsula de Guanahacabibes / Cabo Corrientes	2	20	7	1	1 U/Th on coral	T1 = MIS 5e	Massip, 1936; Zenkovichy and Ionin, 1969; Gutiérrez-Domech and Duarte-Barrientos, 2001; Pérez et al., 2003; Molerio-Leon, 2005; Pajon et al., 2006; Pérez et al., 2008; Cabrera, 2011; Cabrera et al., 2011; Diaz-Guanche et al., 2014)
4	XX	Isla de la Juventud	1	10	10	1	inferred	T1 = MIS 5e	Jennings, 1913; Zenkovichy and Ionin, 1969; Glushankova et al., 1980; Gutiérrez-Domech and Duarte-Barrientos, 2001; Molerio-Leon, 2005; Pérez et al., 2008; Cabrera, 2011; Cabrera et al., 2011
5	XXII	Playa Larga	1	15	15	1	inferred	T1 = MIS 5e	Zenkovichy and Ionin, 1969; Gutiérrez-Domech and Duarte-Barrientos, 2001; Cabrera and Peñalver, 2003; Molerio-Leon,

(*continued on next page*)

Table 1 (*continued*)

Zone	n°	sequence name	Minimum n° level	maximum elevation sequence	Maximum elevation T1	MoE	Dating	Morpho-stratigraphy	Reference
									2005; Cabrera, 2011; Cabrera et al., 2011
5	XXII	Playa Gijon	2?	19	–	–	–	–	Zenkovichy and Ionin, 1969; Gutiérrez-Domech and Duarte-Barrientos, 2001; Cabrera and Peñalver, 2003; Molerio-Leon, 2005; Cabrera, 2011; Cabrera et al., 2011
5	XXIII	Cienfuego	3	78	–	–	–	–	Zenkovichy and Ionin, 1969; Gutiérrez-Domech and Duarte-Barrientos, 2001; Cabrera and Peñalver, 2003; Molerio-Leon, 2005; Cabrera, 2011; Cabrera et al., 2011

paleontological evidence, Vaughan and Spencer (1902) proposed an Oligocene age for the upper reefal terraces at Punta de Maisi and noted that the fossil coral colonies from the lowermost terrace are similar to the one found in modern reefs. Jennings (1913) briefly described the emerged reef at Isle of Pines (now renamed Isla de la Juventud, Fig. 2, Table 1). Vaughan (1914) compared the modern and emerged reefs of Florida with some Cuban sites. The Cabo Cruz sequence, at the SW tip of Cuba Island (Figs. 2, 3, 4), was interpreted by Taber (1931) as evidence for the protracted uplift of the Sierra Maestra. Later, the Punta de Maisi (Figs. 2, 3, 4, Table 1), at the SE tip of Cuba Island raised, again, attention and was considered as Plio-Pleistocene (Woodring, 1954). The post 1960 literature concerning the Cuban sequences of coastal terraces consisted mainly of geomorphic studies (e.g. Ducloz, 1963; Iturralde--Vinent, 1967, 1969a, 1969b, 1977, 1981, 1982, 1994, 2003, 2013; Franco, 1983; Kartashov and Mayo, 1974; Kartashov and Mayo, 1976; Kartashov et al., 1981; Shantzer et al., 1976; Peñalver et al., 1982a, 1982b; Peñalver, 1982; Peñalver et al., 1997, 1998; Pushcharovski, 1988; Cabrera and Peñalver, 2001; Perez-Aragon et al., 2001), or focused on specific landforms such as karstified notches (Molerio-Leon, 2005) or on archaeology (Pajon et al., 2006).

Geogically speaking, the reefal bioconstructions of the lowermost terrace (T1) are grouped into the Late Pleistocene Jaimanitas Formation (Naprstek, 1978; Salomon, 1995; Toscano et al., 1999; Pajon et al., 2006; see map in Muhs et al., 2018). Regressive, coastal clastic deposits overlying the bioconstructions are defined as the La Cabaña Formation (Peñalver et al., 2003). The Jamainitas Formation consists of shallow marine, lagoonal, and reef carbonates (Cabrera and Peñalver, 2001, 2003; Perera and Rojas, 2005; Toscano et al., 1999; Peñalver et al., 2003). The Jaimanitas Formation is widely present along the coast of the Cuba Island and constitutes the foundation for the cities of La Habana and Santiago de Cuba (Figs. 2, 3, 4). The first attempts at absolute dating of the deposits and bioconstructions from the lower T1 coastal terrace, i.e. the Jamainitas Formation, started during the late-70s with ^{14}C dating, which yielded results beyond the limit of the method (Naprstek, 1978; Glushankova et al., 1980). Paleomagnetic dating on the Jaimanitas formation as well as on higher and older terraces has been carried out at Punta de Maisi (Pérez Lazo, 1986; Peñalver et al., 2003) and yielded normal polarities compatible with the correlation of the MIS 5 and MIS 7 highstands with the two lowermost coastal terraces. Older terraces have been dated at 0.8 to 3 Ma (Pérez Lazo, 1986; Peñalver et al., 2003). Coral colonies of the Jamainitas Fm. from coral reef terraces were U/Th dated and correlated to the last interglacial maximum at Matanzas (Toscano et al., 1999) as well as on the NW tip of the Island (Pajon et al., 2006). In NE Cuba, at Matanzas, the Jamainitas Fm (T1) was, again, dated by U/Th and ESR and correlated to MIS 5e in studies of karst systems (De Waele et al., 2017, 2018; Schielein et al., 2020). Finally, in SE Cuba, to the South of the 116 km^2 Guantanamo American Naval Base, fossil coral-colonies forming the bio-constructed part of the lowest coastal terrace, i.e. the Jamainitas Fm., were massively sampled and U/Th dated (> 50 samples). Thirteen dates were considered as reliable and correlated T1 to the last interglacial maximum (MIS 5e; see Table 1 in Muhs et al., 2018).

3. Methods

3.1. Emerged sequences of tropical coastal terraces and uplift estimates

Coastal terraces such as marine, sedimentary, and coral reef terraces forming emerged sequences are stacked fingerprints of the course of sea-level changes on rising coastal realms (Guilcher, 1969; Mesolella et al., 1969; Lajoie, 1986; Pedoja et al., 2011, 2014; Murray-Wallace and Woodroffe, 2014; Rovere et al., 2016). These terraces are, to the first order, associated with Quaternary interglacial sea-level high-stands (Murray-Wallace and Woodroffe, 2014). The shoreline angle is defined as the break of slope between the rockyshore platform or the reef flat and the fossil sea-cliff associated with the terrace (e.g. Lajoie, 1986; Jara-Muñoz et al., 2019), and usually provides a good estimate for the position of the sea level when the terrace was formed (Bull, 1985; Speed and Cheng, 2004).

In tropical environments, coral reef crests and reef flats are not always present alongshore. Some stretches are carved into notches and shore platforms, whereas others include beaches, estuaries and/or mangroves. When present, coral reefs display a variety of morphologies that record the interplay between sea level oscillations and vertical land motion (e.g. Montaggioni and Braithwaite, 2009; Husson et al., 2018; Pastier et al., 2019). Modern and ancient coastal records usually exhibit alongshore variations of erosional landforms, deposits and bio-constructions (Speed and Cheng, 2004; Pedoja et al., 2018). The lowest Cuban coastal terrace T1 perfectly illustrates the interplay between constructional, erosional and depositional processes (Crosby, 1883; Agassiz, 1894; Iturralde-Vinent, 2013). The coastal terrace (Fig. 5) comprises an upgrading fossil reefal unit, the Jamainitas Fm. which is frequently truncated by an erosive surface and overlain by the regressive shingle or sandy beach deposits of the La Cabaña Fm. (Peñalver et al., 2003; Muhs et al., 2018). Such composite landforms are also described at la Désirade (Léticée et al., 2019) and Haiti (Jones, 1918; Woodring, 1954).

We mapped the Cuban sequences of coral reef and marine terraces based on our field observations complemented by the analysis of literature and maps. We measured the elevations of the fossil shoreline angles from topographic maps and/or by the use of various barometrical altimeters. Besides instrumental errors, we assigned a margin of error to all field measurements. The natural rugosity of the landforms is the main source of error; far beyond instrumental errors. The roughness of the landforms increases with elevation and age. For low-standing landforms, the margin of error is set to ±1 m whereas for upper strandlines it

Table 2
Apparent and eustasy-corrected corrected uplift rates of the Cuban Archipelago. All the rates and associated errors are in mm.yr^{-1} or m.ka^{-1}. The estimates vary in function of the eustatic range yielded by various methods.

N°	Area	Sequence n°	Site name	Terrace	Chrono-stratigraphy	Dating method	Reference	Elevation strandline / landform		Age MIS		Apparent uplift rates				Eustatic correction Murray-Wallace and Woodroffe (2014)		Corrected uplift rate Murray-Wallace and Woodroffe (2014)			
								Es	MoE	age	MoE	U max	U min	U mean	MoE	e	MoE	U max	U min	U mean	MoE
1	1	IV	Guantanamo light house	T1	MIS 5e	U/Th on coral	Muhs et al., 2018	15	1	122	6	0.14	0.11	0.12	0.02	6	4	0.12	0.03	0.08	0.04
2	1	IV	Guatanamo bay	T1	MIS 5e	U/Th on coral	Muhs et al., 2018	10.8	1	122	6	0.1	0.08	0.09	0.01	6	4	0.08	0	0.04	0.04
3	1	VI	Peninsula Maisi	T1	MIS 5e	paleomagnetism	Pérez Lazo, 1986; Peñalver et al., 2001; Peñalver et al., 2003	15	1	122	6	0.14	0.11	0.12	0.01	6	4	0.12	0.03	0.08	0.04
4	1	VI	Peninsula Maisi	T1	MIS 5e	paleomagnetism	Pérez Lazo, 1986; Peñalver et al., 2001; Peñalver et al., 2003	40	1	122	6	0.35	0.3	0.33	0.01	6	4	0.34	0.23	0.28	0.05
5	2	IX	Banes	T1	MIS 5e	inferred	This study	15	1	122	6	0.14	0.11	0.12	0.02	6	4	0.12	0.03	0.08	0.04
6	2	X	Ciego de Avila SE	T1	MIS 5e	inferred	This study	10	1	122	6	0.09	0.07	0.08	0.01	6	4	0.08	−0.01	0.03	0.04
7	2	XI	Ciego de Avila Cayos	T1	MIS 5e	inferred	This study	8	1	122	6	0.08	0.05	0.07	0.02	6	4	0.06	−0.02	0.02	0.04
8	2	XII	Ciego de Avila NE	T1	MIS 5e	inferred	This study	10	1	122	6	0.09	0.07	0.08	0.01	6	4	0.08	−0.01	0.03	0.04
9	2	XIII	Cayo Santa Maria	T1	MIS 5e	inferred	This study	12	1	122	6	0.11	0.09	0.1	0.01	6	4	0.09	0.01	0.05	0.04
10	3	XIV	Varadero – Carbonera	T1	MIS 5e	inferred	This study	19	1	122	6	0.17	0.14	0.16	0.02	6	4	0.16	0.06	0.11	0.05
11	3	XV	Matanzas	T1	MIS 5e	U/Th on speleothem	De Waele et al., 2017; De Waele et al., 2018	16	1	122	6	0.15	0.12	0.13	0.02	6	4	0.13	0.04	0.08	0.05
12	3	XVIII	Mariel- Harlem	T1	MIS 5e	inferred	This study	7	1	122	6	0.07	0.05	0.06	0.01	6	4	0.05	−0.03	0.01	0.04
13	4	XIX	Cabo Corrientes	T1	MIS 5e	U/Th on coral	Pajon et al., 2006	7	1	122	6	0.07	0.05	0.06	0.01	6	4	0.05	−0.03	0.01	0.04
14	4	XX	Isla de la Juventud	T1	MIS 5e	inferred	This study	10	1	122	6	0.09	0.07	0.08	0.01	6	4	0.08	−0.01	0.03	0.04
15	5	XXI	Camilo Cienfuego	T1	MIS 5e	inferred	This study	15	1	122	6	0.14	0.11	0.12	0.02	6	4	0.12	0.03	0.08	0.04

Es elevation strandline. *Age MIS*: age of the marine isotopic stage. *e*: eustatic correction. *U max*:maximal uplift rate. *U min*: minimal uplift rate. *U mean*: mean uplift rate.

reaches ±10 m because of increased erosion and karstification with age and elevation, as observed in the field.

3.2. Pleistocene sea-level curves, uplift rates, Holocene relative sea-level

Taking into account previous dating, we derive Upper Pleistocene uplift rates (Table 2) based on the elevation of the coastal terraces allocated to the Last Interglacial Maximum, MIS 5e (122 ± 6 ka). Eustasy-corrected or absolute uplift rates are given by dividing the difference between the present elevation of the shoreline angle and the eustatic sea-level at its formation time by the age of the terrace (Lajoie, 1986).

Apparent (or relative) uplift rates neglect any *priori* eustatic correction (as in Pedoja et al., 2011, 2014, 2018; Yildirim et al., 2013; Authemayou et al., 2016). Correcting for eustasy requires some knowledge of the absolute sea level at the time of construction of the marine terrace. Many sea-level curves have been derived from the oxygen isotopic records (Shackleton, 1987; Waelbroeck et al., 2002; Lisiecki and Raymo, 2005; Bintanja and Van de Wal, 2008; Zachos et al., 2008; Rohling et al., 2009, see de Gelder et al., 2020 for details on these curves), but also from -or combined to- the geomorphologic record (Siddal et al., 2006; Murray-Wallace and Woodroffe, 2014). These sea-level curves frequently present discrepancies in the ages and elevation of MIS highstands (Table 2; see Caputo, 2007; Murray-Wallace and Woodroffe, 2014; de Gelder et al., 2020), but there is a relative consensus on the succession of the most recent high-stands. The most common high-stands in the geomorphological record are those related the last interglacial period, MIS 5 (Johnson and Libbey, 1997; Stirling et al., 1998; Pedoja et al., 2011; Murray-Wallace and Woodroffe, 2014), which includes three relative high-stands, MIS 5a (85 ± 5 ka), MIS 5c (105 ± 5 ka) and MIS 5e (128 ka to 116 ka). The MIS 5e highstand corresponds to the last interglacial maximum; it displays one to three coastal terraces in nearly all the studied sequences worldwide and constitutes a common benchmark (Pedoja et al., 2011, 2014; Murray-Wallace and Woodroffe, 2014).

In order to account for the variability of sea-level curves, we analyzed the sequences of the Cuban Archipelago considering a recent compilation of geomorphic indicators (Murray-Wallace and Woodroffe, 2014) but also five eustatic curves (Table 2, Waelbroeck et al., 2002; Bintanja and Van de Wal, 2008; Grant et al., 2014; Shakun et al., 2015; Spratt and Lisiecki, 2016). Murray-Wallace and Woodroffe (2014) consider that MIS 5e, MIS 7, MIS 9, and MIS 11 highstands were respectively at 6 ± 4 m, −8 ± 12 m, 3 ± 2 m, and 9.5 ± 3.5 m with respect to present-day sea level (Table 2). The five sea-level curves (see Table 2 for more details) were selected to encompass five different reconstruction methods, to cover the time-range of interest and to have quantified uncertainties (Waelbroeck et al., 2002; Bintanja and Van de Wal, 2008; Grant et al., 2014; Shakun et al., 2015; Spratt and Lisiecki, 2016). These different estimates of past sea levels convert into different estimates of uplift rates (e.g. de Gelder et al., 2020).

Contrarily, to the Indo-Pacific, the Caribbean has no mid-Holocene highstand (Fig. 5C) as evidenced by the documented monotonic rise in Holocene sea level and explained by Glacial Isostatic Adjustment models (Fairbridge, 1961; Clark et al., 1978; Khan et al., 2017).

Eustatic correction Waelbroeck et al. (2002)		Corrected Uplift rate Waelbroeck et al. (2002)				Eustatic correction Bintanja and Van der Wal (2008)		Corrected Uplift rate Bintanja and Van der Wal (2008)				Eustatic correction Grant et al. (2014)		Corrected Uplift rate Grant et al. (2014)				Eustatic correction Shakun et al. (2015)		Corrected Uplift rate Shakun et al. (2015)				Eustatic correction Spratt and Lisiecki (2016)			Corrected Uplift rate Spratt and Lisiecki (2016)			
e	MoE	U max	U min	U mean	MoE	e	MoE	U max	U min	U mean	MoE	e	MoE	U max	U min	U mean	MoE	e	MoE	U max	U min	U mean	MoE	e	Moe (+)	MoE (−)	U max	U min	U mean	MoE
6	13	0.2	−0.04	0.08	0.12	0	8	0.21	0.05	0.13	0.08	5	14	0.22	−0.04	0.09	0.13	−10	10	0.31	0.11	0.21	0.1	3	12	20	0.22	−0.07	0.07	0.14
6	13	0.16	−0.07	0.05	0.12	0	8	0.17	0.01	0.09	0.08	5	14	0.18	−0.07	0.05	0.13	−10	10	0.27	0.08	0.18	0.1	3	12	20	0.18	−0.1	0.04	0.14
6	13	0.2	−0.04	0.08	0.12	0	8	0.21	0.05	0.13	0.08	5	14	0.22	−0.04	0.09	0.13	−10	10	0.31	0.11	0.21	0.1	3	12	20	0.22	−0.07	0.07	0.14
6	13	0.41	0.16	0.29	0.13	0	8	0.42	0.24	0.33	0.09	5	14	0.43	0.16	0.29	0.14	−10	10	0.53	0.3	0.42	0.11	3	12	20	0.43	0.13	0.28	0.15
6	13	0.2	−0.04	0.08	0.12	0	8	0.21	0.05	0.13	0.08	5	14	0.22	−0.04	0.09	0.13	−10	10	0.31	0.11	0.21	0.1	3	12	20	0.22	−0.07	0.07	0.14
6	13	0.16	−0.08	0.04	0.12	0	8	0.16	0.01	0.09	0.08	5	14	0.17	−0.08	0.05	0.13	−10	10	0.27	0.07	0.17	0.1	3	12	20	0.17	−0.11	0.03	0.14
6	13	0.14	−0.09	0.02	0.12	0	8	0.15	−0.01	0.07	0.08	5	14	0.16	−0.09	0.03	0.12	−10	10	0.25	0.05	0.15	0.1	3	12	20	0.16	−0.13	0.02	0.14
6	13	0.16	−0.08	0.04	0.12	0	8	0.16	0.01	0.09	0.08	5	14	0.17	−0.08	0.05	0.13	−10	10	0.27	0.07	0.17	0.1	3	12	20	0.17	−0.11	0.03	0.14
6	13	0.17	−0.06	0.05	0.12	0	8	0.18	0.02	0.1	0.08	5	14	0.19	−0.06	0.06	0.13	−10	10	0.28	0.09	0.19	0.1	3	12	20	0.19	−0.09	0.05	0.14
6	13	0.23	−0.01	0.11	0.12	0	8	0.24	0.08	0.16	0.08	5	14	0.25	−0.01	0.12	0.13	−10	10	0.34	0.14	0.24	0.1	4	13	21	0.25	−0.05	0.1	0.15
6	13	0.21	−0.03	0.09	0.12	0	8	0.22	0.05	0.14	0.08	5	14	0.22	−0.03	0.1	0.13	−10	10	0.32	0.12	0.22	0.1	3	12	20	0.22	−0.06	0.08	0.14
6	13	0.13	−0.1	0.01	0.12	0	8	0.14	−0.02	0.06	0.08	5	14	0.15	−0.1	0.02	0.12	−10	10	0.24	0.05	0.14	0.1	3	12	20	0.15	−0.13	0.01	0.14
7	13	0.12	−0.11	0.01	0.12	0	8	0.14	−0.02	0.06	0.08	5	14	0.15	−0.1	0.02	0.12	−10	10	0.24	0.05	0.14	0.1	3	12	20	0.15	−0.13	0.01	0.14
6	13	0.16	−0.08	0.04	0.12	0	8	0.16	0.01	0.09	0.08	5	14	0.17	−0.08	0.05	0.13	−10	10	0.27	0.07	0.17	0.1	3	12	20	0.17	−0.11	0.03	0.14
6	13	0.2	−0.04	0.08	0.12	0	8	0.21	0.05	0.13	0.08	5	14	0.22	−0.04	0.09	0.13	−10	10	0.31	0.11	0.21	0.1	3	12	20	0.22	−0.07	0.07	0.14

4. The Cuban sequences of coastal terraces

The Cuban archipelago and continental platform (Figs. 2, 3, 4, 5) exhibit five main areas of emerged coastal terrace sequences (Table 1). These uplifting coastal stretches are separated by subsiding areas (Iturralde-Vinent, 2013; Fig. 5). In total, we collected quantitative data for 23 sequences (Fig. 3, Table 1) that generally correspond to staircase coastal landscapes including up to four successive strandlines.[1] The most complete sequences, in terms of successive fossil shorelines, are preserved on the SE and SW tips of Cuba Island (sequences I and V, VI, VII Table 1 Figs. 3, 4). Submerged sequences of terraces are mentioned to the N and SE of the Cuban Archipelago (Fig. 5).

The uplifting coastal stretch n°1 (sequences I to VIII, Table 1, Figs. 3, 4) corresponds to the whole southern coast of Cuba Island, from Nibujón (Baracoa district) in the East, to Cabo Cruz in the West. Along this ~500 km long coastal stretch, we identified eight sequences. In agreement with previous observations (e.g. Pérez et al., 2011), we observed that the lowest coastal terrace (T1) is almost continuous over 350 km, from Santiago de Cuba to Baracoa (Figs. 2, 3, 4). Between West Santiago de Cuba and East Cabo Cruz (Fig. 2), the coast is characterized by plunging sea-cliffs and no sequences of coral reef and marine terraces are present (Cabrera and Peñalver, 2003; Iturralde-Vinent, 2013). At the Guantanamo USA naval base, coral colonies from the lowermost terrace were previously U/Th dated and correlated to the last Interglacial (sequence n°IV, Table 1 and Section 2.2). Nevertheless, all along South Cuba, the shoreline angle of the lowermost coastal terrace, that we infer to relate to MIS 5e, is emplaced at elevations that still have to be determined more accurately, and needs to be dated to confirm this inference (Muhs et al., 2018). The SW and SE tips of Cuba Island, Cabo Cruz and Punta de Maisi respectively, exhibit well-preserved sequences of marine and coral reef terraces (Fig. 6). To the SW, the Cabo Cruz sequence (sequence I, Table 1, Figs. 3, 4) reaches 263 ± 10 m and includes 13 coastal terraces and an unknown number of associated notches. Cabo Cruz is referred to as a major natural site for world heritage by UNESCO[2] but the bioconstructions associated to the successive terraces of this impressive sequence[3,4] are not yet dated. On Punta de Maisi (sequence VI, Table 1, Figs. 3, 4, 6), the sequence reaches a maximum elevation of 560 ± 10 m, includes 24 coastal terraces and an unknown number of associated notches. There, the two lowermost coastal terraces are raised at elevations ranging from 15 to 40 m for T1 and from 25 to 60 m for T2 and have been correlated to MIS 5 and MIS 7 highstands in paleomagnetic studies (Section 2.2.). Here, we assign the lowest terrace T1 to MIS 5e, akin to other Cuban coastal sites, and also because it yields the lowest, or minimum uplift rates for the last interglacial as the last interglacial maximum is the oldest highstand of this MIS with the highest eustatic sea-level. At other sites of the Cuban South shore, such as Siboney and

[1] https://youtu.be/cBRfgm9c-pI

[2] https://whc.unesco.org/en/list/889/

[3] https://youtu.be/7I9mK8a_bI8

[4] https://youtu.be/vW_zErZWMDc

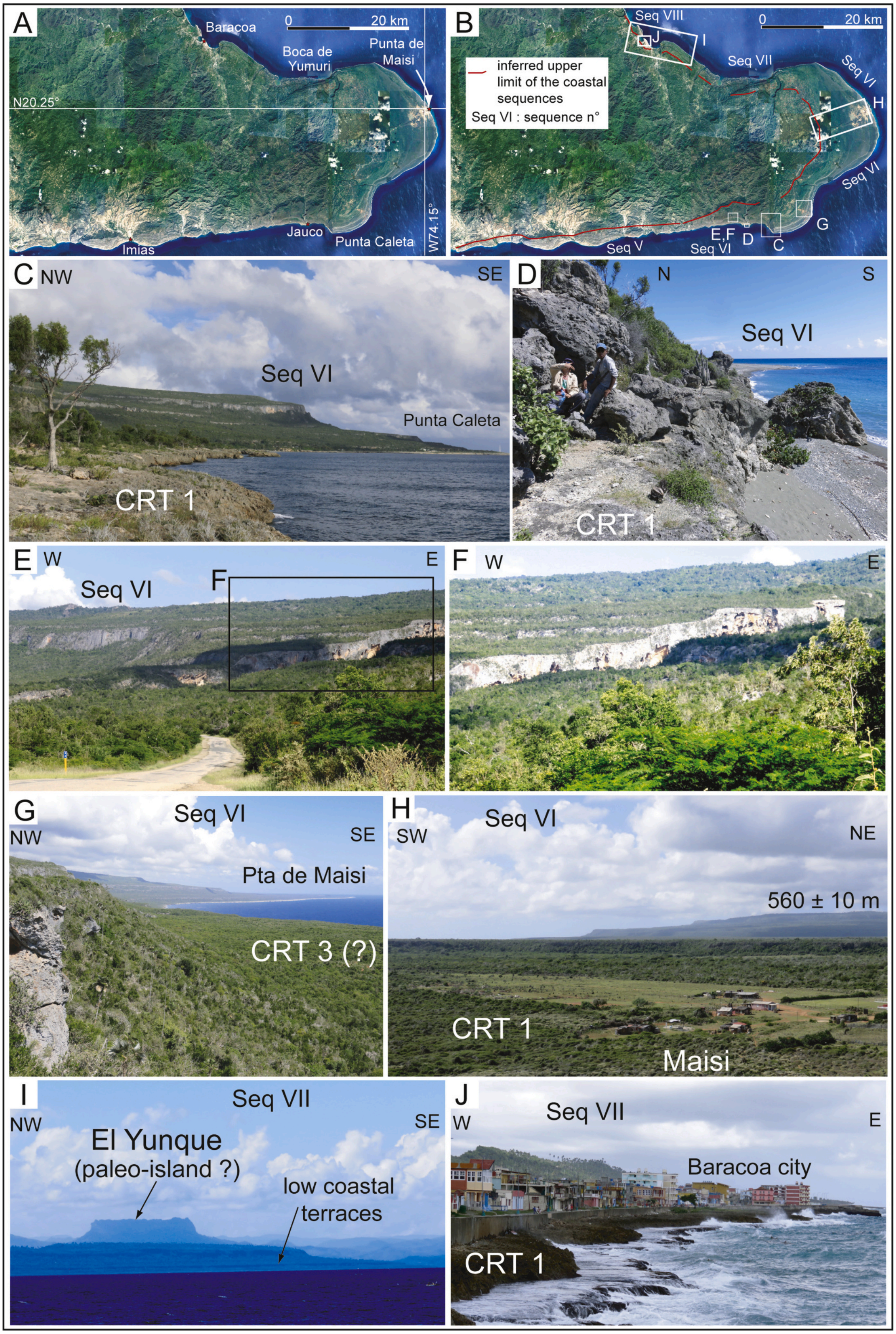

Fig. 6. The coastal sequences between Imias and Baracoa, Oriente, Cuba. A) Toponymy B) Sequences distribution C) The Punta Caleta sequence D) The lowest coastal terrace at Jauco E), F) Incised sequence G) The Punta Caleta sequence H) The Punta de Maisi sequence as seen from the lighthouse I) The East Baracoa sequence. J) The lower terrace at Baracoa. CRT coral reef terrace, Pta Punta, Sequ. Coastal sequence.

Juragua, the sequences include 3 to 4 successive shorelines[5,6,7] (sequence II, III, V Table 1, Figs. 3, 4). The uplifting southern shore of Cuba (area 1) is delimited to the North by the subsiding Guacanoyabo-Nipe tectonic corridor (Fig. 4).

The uplifting coastal stretch n°2 (sequences IX to XII Table 1, Figs. 3, 4) is ~420 km long and includes the rocky islets (*cayos*) of the Sabana - Camaguey Archipelago (Fig. 2) as well as a part of the NW-SE trending shore of the NE side of Cuba island (sequence XII, Table 1, Figs. 3, 4). In this area, a single terrace has its shoreline angle raised at elevations ranging from 8 ± 1 m to 15 ± 1 m (Table 1, Fig. 3). Northwards, the uplifting coastal stretch ends on the Caibarién Fault, which separates it from the second subsiding area. Northwards, this subsiding area is limited by another major fault: the NS trending Cochinos - Cardenas Fault which also affects the fifth area exhibiting emerged coastal sequences (Figs. 3, 4).

The uplifting coastal stretch n°3 extends from Varadero to Bahia Onda (sequences XIV to XVIII, Table 1, Figs. 2, 3) over ~240 km and includes the Matanzas sequence (n°XV Fig. 3, Table 1). The central part of this coastal stretch exhibits sequences with up to 3 coastal terraces, reaching maximum elevations of 100 ± 10 m. The sequences located eastwards (sequence XIV) and westwards (sequence XVIII) of the central part exhibit only a single coastal terrace. The shoreline angle of T1 is emplaced at higher elevation (19 ± 1 m at sequence XIV) in the East than in the West (7 ± 1 m at sequence XVIII). At Matanzas, the lowest T1 terrace, dated and correlated to MIS 5e (Section 2.2.) has its shoreline angle raised at 16 ± 1 m. This uplifting coastal stretch is parallel to the Pinar Fault and separated from the fourth area of coastal sequences by the subsiding Batanao Gulf (Figs. 3, 4).

The 240 km long uplifted coastal stretch n°4 festoons the NW tip of Cuba island (sequence XIX, Table 1, Figs. 3, 4) as well as the southern shore of La Juventud Island (sequence XX, Table 1, Fig. 3). On the NW tip of Cuba (sequence XIX and XX, Table 1, Fig. 3), the sequences include two successive coastal terraces up to 20 ± 1 m in elevation whereas on La Juventud Island a single terrace is preserved at 10 ± 1 m (Table 1, Fig. 3).

The subsiding Batanao Gulf (Fig. 4) delimits, to the NW, the uplifting coastal stretch n° 5 (sequence XXI to XXIII, Table 1, Fig. 3) which extends on the central part of South Cuba over 200 km. Within this area, the Cochinos - Cardenas Fault perpendicularly crosscuts the modern coastline. To the West of the fault, sequence XXI includes a single coastal terrace for which the shoreline angle is preserved at 15 ± 1 m, while eastwards, the sequences XXII and XXIII include up to three successive shorelines, and reaches 78 ± 1 m at sequence XXIII (Table 1, Fig. 3). At sequence XXI, the distribution of the coastal terrace suggests the occurrence of a paleo-gulf as the fossil shoreline enters inland, unlike its modern counterpart. To the East, the fifth uplifting coastal stretch ends at the La Trocha Fault (Fig. 4), which borders the SW subsiding areas of the Cuban Archipelago.

The elevation and distribution of the coastal sequences of the Cuban archipelago depict nine units with different tectonic behavior intimately related with onshore and offshore faults (Fig. 4). Five blocks are uplifting and four subsiding. The blocks are generally delimited by onshore faults associated with a vertical component, generally normal except the Cochinos-Cardenas reverse fault, and for some with strike-slip component, particularly Cauto-Nipe and La Trocha (Fig. 4; Garcia, 2001). The uplifted sections are characterized by coastal sequences with different morphologies revealing variable Upper Pleistocene (MIS 5e) uplift rates and Late Cenozoic emersion histories (Fig. 4).

[5] https://youtu.be/hFLFR8i4kyo
[6] https://youtu.be/6HwpmNV5538
[7] https://youtu.be/GDuZqlRjNpk

5. Discussion

5.1. Estimates of Upper Pleistocene uplift rates and timing for the emersion of some sequences of coastal terraces

Most of the Cuban coastal terraces allocated to the Last Interglacial Maximum (MIS 5e) are found at lower elevations than 20 m (Table 2), which implies low to very low apparent uplift rates (Class C and D, Fig. 4 in Pedoja et al., 2011) ranging from 0.06 ± 0.01 mm.yr^{-1} on the NW tip of Cuba main island (sequence XIX) to 0.13 ± 0.01 mm.yr^{-1} at Matanzas (sequence XV, Table 1, Fig. 4). At Punta de Maisi (sequence VI, Table 1), the shoreline angle of the MIS 5e reefal terrace is emplaced at a maximum elevation of 40 ± 1 m (Pérez Lazo, 1986; Peñalver et al., 2003) which implies a moderate apparent coastal uplift rate of 0.33 ± 0.01 mm.yr^{-1} (Class B on Fig. 4 in Pedoja et al., 2011). On the southern part of the US Naval base of Guantanamo Bay, MIS 5e apparent uplift rates are low with values of 0.12 ± 0.02 mm.yr^{-1} (Guantanamo Lighthouse Table 1) in the exposed area and of 0.09 ± 0.02 mm.yr^{-1} in the protected area (Guantanamo Bay Table 1).

As the MIS 5e landform is generally low (< 20 m), eustasy-corrected uplift rates are more variable since the rates largely depend on the correction applied (Table 2). Within the Guantanamo embayment, the shoreline angle of the reefal terrace correlated to the MIS 5e is emplaced at 10.8 ± 1 m which yields uplift rates of 0.05 ± 0.12 mm.yr^{-1} (following Waelbroeck et al., 2002) or 0.18 ± 0.10 mm.yr^{-1} (following Shakun et al., 2015). Upon some sea-level curves and taking into account the large margins of error, uplift rates can even be negative, and therefore the MIS 5e terrace interpreted as evidence of subsidence (Table 2), although this would be at odds with the accompanying sequences of coastal landforms that attest for an overall uplift.

Assuming constant apparent uplift rates, we extrapolated the apparent MIS 5e uplift rates to propose a possible age for the uppermost shorelines of some sequences (as in Lajoie, 1986). These extrapolations provide an indicative chronological framework. Extrapolating eustasy-corrected uplift rates would yield older emersion age for the considered sequences. Extrapolating an apparent MIS 5e uplift rate of 0.13 ± 0.01 mm.yr^{-1}, the summit of the Matanzas sequence (n° XV Fig. 3) at 100 ± 10 m would have emerged between 640 ka and 910 ka, during middle or early Pleistocene time (Fig. 4). The more complete sequences of Maisi (560 ± 10 m) and Cabo Cruz (263 ± 10 m) seem to represent longer periods of time, probably since Pliocene in agreement with paleomagnetic dating indicating ages of 3 Ma at Punta de Maisi (Section 2.2). Consequently at Maisi and Cabo Cruz, the long-lasting records of sea-level fluctuations are intermediary steps between the ~1 Ma coastal sequences preserved on Barbados or Sumba island (Indonesia) and the long lasting sequence of Buton Island (SE Sulawesi, Indonesia) which probably record 3.8 ± 0.6 Ma (Fig. 15 Pedoja et al., 2018 for a graphical representation of the long lasting reefal sequences mentionned here).

5.2. Tectonic implications

Within the current state of the art regarding Cuban coastal sequences, as intuitively suspected the highest apparent or eustasy-corrected Upper Pleistocene coastal uplift rates from dated reefal terraces (maximum of 0.33 ± 0.01 mm.yr^{-1}) are located next to the transform zone, at Punta de Maisi (sequence V, Table 1, Fig. 3). We stress that there are no dating and/or elevations measurements for the Cabo Cruz sequence (sequence I, Table 1, Figs. 3, 4) also located next to the Transform Fault Zone and which might reveal similar or stronger Upper Pleistocene uplift rates than at Punta de Maisi.

Cuban coastal sequences evidence non-negligible uplift of NW Cuba Island (sequences XV, Fig. 2B), more than 400 km to the North of the Oriente Transform Fault Zone. Such coastal uplift is probably the aftermath of the tilting of tectonic blocks, associated with *E*-W-trending faults crossing the Cuban platform (Figs. 1, 4). Some uplifting coastal stretches are obviously tilted or warped like Area 3 (Fig. 3) and the

Punta de Maisi. Within the uplifting coastal stretch n°3, the T1 shoreline angle elevation yields higher apparent uplift rates in the East (sequence XIV, 0.16 ± 0.02 mm.yr^{-1}) than in the West (sequence XVIII, 0.06 ± 0.01 mm.yr^{-1}). Not taking into account the Punta de Maisi, the highest Upper Pleistocene apparent coastal uplift rates are those determined some 190 km North of the Transform Fault Zone at or near Matanzas (sequence XIV and XV, respectively 0.16 ± 0.02 mm.yr^{-1} and 0.13 ± 0.01 mm.yr^{-1}, Tables 1, 2, Fig. 3), similar or slightly higher than the uplift rates experienced by the south coast of Guantanamo U.S. Military Naval Base (0.12 ± 0.02 mm.yr^{-1}), 35-km North of the Oriente Transform Fault.

In the eastern part of the northern Caribbean transform plate boundary, shortening occurs due to the obliquity of plate convergence. The transition from a transform to a subduction plate boundary implies the Bahamas bank collision to the North and the Beata ridge indentation to the South (Mann and Burke, 1984; Mann et al., 1995, 2005; Rojas-Agramonte et al., 2005; Symithe et al., 2005; Calais et al., 2016; Corbeau et al., 2019; Wessels et al., 2019) (Fig. 1). Uplift of some stretches of the Cuban coasts suggests that compression might affect areas located as far as 400 km North of the Transform Fault, probably through (re-)activation of Paleocene-Eocene strike-slipe faults with some vertical motion components, like the Caute-Nipe, La Trocha and Pinar Faults. Major sinistral transpressive deformations associated with folding and thrusting has been described all across Hispaniola island with various proxies: bathymetry and seismic reflection profiles across the western basins (Calais and Mercier De Lépinay, 1995; Leroy et al., 2015; Corbeau et al., 2016), geological cross-sections (Pubellier et al., 2000; Escuder-Viruete et al., 2020), seismicity (Calais et al., 2010; Possee et al., 2018; Corbeau et al., 2019), paleoseismicity (Bakun et al., 2012; Prentice et al., 2010); and GPS networks (Benford et al., 2012; Symithe et al., 2005; Calais et al., 2016). Coastal uplift seems to be higher in Haiti, where impressive sequences are present in the Northwest of Hispaniola Island (Dodge et al., 1983). In NW Haiti, the shoreline angle of MIS 5e coral reef terrace reaches 60 m which yields an apparent uplift rate of ~0.5 mm.yr^{-1} (Dumas et al., 2006) although these results have been commented (Hearty et al., 2007).

East of the Caribbean area, the most studied sequence of coastal terraces is the one present on Barbados Island located ~1700 km SE of SE Cuba (Fig. 1). The island, an uplifting accretionary prism at the front of the Lesser Antilles subduction zone, exhibits a staircase sequence which reaches 300 +/− 10 m in elevation, includes 13 main coastal terraces, and represents ~1 Ma of sea-level fluctuations. The MIS 5e shoreline angle is raised at a maximum elevation of 41 ± 1 m (Radtke and Schellmann, 2006; Potter et al., 2004; Schellmann and Radtke, 2004; Schellmann et al., 2004; Thompson et al., 2003; Villemant and Feuillet, 2003; Gallup et al., 2002; Johnson, 2001; Muhs, 2001), yielding apparent uplift rates of 0.33 ± 0.01 mm.yr^{-1}. Such rates are comparable to those determined herein, for the Punta de Maisi, in SE Cuba, just in front of the Transform Fault Zone. However, at la Desirade Island, in front of the Caribbean subduction zone at a location where the accretionary prism is less developed, the shoreline angle of the coastal terrace allocated to the last interglacial maximum (MIS 5e, 122 ± 6 ka) lies at 10 ± 1 m (Léticée et al., 2019). This yields an apparent uplift rate of 0.08 ± 0.01 mm.yr^{-1} equivalent to the upper Pleistocene coastal uplift rates in NE Cuba, ~ 190 km from the Transfom Fault Zone. The scarcity of dating of Pleistocene coastal landforms for the impressive sequences of South Cuba and West Haiti, which are higher in elevation and more complete in terms of successive terraces than the canonical Barbados sequence, avoid us from having detailed Pleistocene vertical motions and, overall, better constrained coastal uplift rates for the Caribbean area.

Considering a database made by members of our team (Pedoja et al., 2014), at a global scale, within transform tectonics settings, the MIS 5e benchmark is recorded at i) 121 sites of which 3 are submerged, ii) MIS 5e shoreline angles are found at elevations ranging from - 5 ± 5 m (Belize Island) to 275 ± 25 m (at Smith Gulf, California) with a mean of ~30.5 ± 3 m, and iii) the mean Late Pleistocene apparent uplift rate of Transform settings is 0.25 ± 0.02 mm.yr^{-1}. Such values would be probably slighlty different considering more recent databases on the MIS 5e shoreline elevation and other sea level proxies in the Caribbean area (Rubio-Sandoval et al., 2021; Simms, 2021) but the latter do not include geodynamical data. Nevertheless, in theory, purely transform settings do not cause vertical land motion, which is in practice seldom observed. On coasts located in front of intra-oceanic subduction zones, the elevation of MIS 5e shorelines range from −85 ± 2.5 m to 240 ± 3 m with a mean of ~51.3 ± 3.1 m. The mean Late Pleistocene apparent coastal uplift rate is 0.42 ± 0.03 mm.yr^{-1} (Pedoja et al., 2014). The Lesser Antilles Fault Zone exhibits relatively low Upper Pleistocene uplift rates when compared to similar settings (subduction Mariana type). The apparent Late Pleistocene uplift rates experienced at the SE tip of Cuba (Maisi Peninsula, 0.33 ± 0.01 mm.yr^{-1}) or Haiti, are typical of Transform Fault Zone settings. Transform Fault zones frequently experience positive vertical deformations in relation to, among other, plate convergence obliquity, mantle flow and/or the rotation of crustal blocks. The relative contribution of these processes responsible for the Late Cenozoic uplift of the Cuban coasts still has to be determined.

6. Conclusion

The Late Cenozoic coastal evolution of the Cuban Archipelago includes the uplift of five coastal stretches, recorded by 23 emerged sequences of coastal terraces. MIS 5e terraces (122 ± 6 ka) are found at elevations lower than 20 m, except at Punta de Maisi in front of the Oriente Transform Fault Zone where it is raised at a maximum elevation of 40 ± 1 m. Consequently, upper Pleistocene apparent coastal uplift rates range from 0.06 ± 0.01 mm.yr^{-1} to the NW of Cuba Island to 0.33 ± 0.01 mm.yr^{-1} in front of the Oriente Transform Fault Zone. Coastal uplift distribution shows that deformation is active up to 400 km North of the Transform Fault Zone. Long lasting sequences of notches, marine and coral reef terraces are preserved on the southern tips of Cuba Island at Punta de Maisi (SE) and Cabo Cruz (SW), in front of the Transform Fault Zone. At Maisi the sequence of 24 coastal terraces reaches 560 ± 10 m in elevation and represent a ~ 3 Ma record of sea-level fluctuations assuming constant uplift rates. On Cabo Cruz, the poorly studied sequence of 13 coastal terraces reaches 263 ± 10 m in elevation but there are no dating nor precise elevations of the successive terraces and notches. Future dating of the Cuban coastal terraces will shed light on regional tectonics and on Pleistocene coastal morphogenesis in an area, a priori less exposed to Holocene sea level variations than other regions.

Declaration of Competing Interest

None.

Acknowledgments

This work was supported by ISblue Project, Interdisciplinary Graduate School for the Blue Planet (ANR-17-EURE-0015) and co-funded by a grant from the French government under the program "Investissements d'Avenir" (VuCoREm, Authemayou) and the CNES TOSCA Program (CETTROPICO, C. Authemayou). We thank Mary Elliot for her polishing and bettering of our manuscrit. We thank all the coastal dwellers who shared their knowledge with us.

References

Agassiz, A., 1894. A Reconnoissance of the Bahamas and of the Elevated Reefs of Cuba in the Steam Yacht" Wild Duck", January to April 1893, Museum.
Alexander, C.S., 1961. The marine terraces of Aruba, Bonaire, and Curacao, Netherlands Antilles. Ann. Assoc. Am. Geogr. 51 (1), 102–123.
Alvarez, L., Lindholm, C., Villalon, M., 2017. Seismic hazard for Cuba: a new approachseismic hazard for Cuba: a new approach. Bull. Seismol. Soc. Am. 107 (1), 229–239.

Authemayou, C., Pedoja, K., Heddar, A., Molliex, S., Boudiaf, A., Ghaleb, B., Lanoe, B.V. V., Delcaillau, B., Djellit, H., Yelles, K., 2016. Coastal uplift west of Algiers (Algeria): pre-and post-Messinian sequences of marine terraces and rasas and their associated drainage pattern. Int. J. Earth Sci. 1–23.
Bakun, W.H., Flores, C.H., ten Brink, U.S., 2012. Significant earthquakes on the Enriquillo fault system, Hispaniola, 1500-2010: implications for seismic hazard. Bull. Seismol. Soc. Am. 102 (1), 18–30.
Benford, B., DeMets, C., Calais, E., 2012. GPS estimates of microplate motions, northern Caribbean: evidence for a Hispaniola microplate and implications for earthquake hazard. Geophys. J. Int. 191 (2), 481–490.
Berry, L., Whiteman, J., Bell, S.V., 1966. Some radiocarbon dates and their geomorphological significance, emerged reef complex of the Sudan. Z. Geomorphol. 10, 119–143.
Bintanja, R., Van de Wal, R.S.W., 2008. North American ice-sheet dynamics and the onset of 100,000-year glacial cycles. Nature 454 (7206), 869–872.
Broecker, W.S., Thurber, D.L., Goddard, J., Ku, T.-l., Matthews, R.K., Mesolella, K.J., 1968. Milankovitch hypothesis supported by precise dating of coral reefs and deep-sea sediments. Science 159 (3812), 297–300.
Brunt, M.A., Giglioli, M.E.C., Mather, J.D., Piper, D.J.W., Richards, H.G., 1973. The Pleistocene rocks of the Cayman Islands. Geol. Mag. 110 (3), 209–221.
Budd, A.F., 2000. Diversity and extinction in the Cenozoic history of Caribbean reefs. Coral Reefs 19 (1), 25–35.
Bull, W.B., 1985. Correlation of flights of global marine terraces. In: 15th Annual Geomorphology Symposium, State University of New York at Binghampton, Hemel Hempstead.
Burke, K., 1988. Tectonic evolution of the Caribbean. Annu. Rev. Earth Planet. Sci. 16 (1), 201–230.
Cabrera, M., 2011. Los depositos cuaternarios del territorio marino de Cuba. Miner. Geol. 27 (3), 1–25.
Cabrera, M., Peñalver, L., 2001. Contribucion a la estratigrafia de los depositos cuaternarios de Cuba. Rev. Cuater. Geomorfol. 15 (3–4), 37–49.
Cabrera, M., Peñalver, L.L., 2003. Contribucion a la estratigrafia de la formacion Jaimanitas y su relacion estratigrafica con las demas formaciones del Pleistoceno superior. Memor. GEOMIN 11–17.
Cabrera, M., Orbera, L., Nuñez, A., Pantaleon, G., Nuñez, K., Triff, J., Pérez, C.M., Santos, M.R., Chavez, M.E., Gonzalez, D., 2011. Movimientos neotectonicos y ascenso del nivel medio del mar en Cuba. Boletín trimestral publicado por el Centro Nacional de Información Geológica del Instituto de Geología y Paleontología 2, 1–16.
Calais, E., Mercier De Lépinay, B., 1995. Strike-slip tectonic processes in the northern Caribbean between Cuba and Hispaniola (Windward Passage). Mar. Geophys. Res. 17 (1), 63–95.
Calais, E., Mercier de Lepinay, B., Saint-Marc, P., Butterlin, J., Schaaf, A., 1992. La Limite de plaques decrochante nord caraibe en Hispanolia; evolution paleogeographique et structurale cenozoique. Bull. Soc. Géol. France 163 (3), 309–324.
Calais, E., Freed, A., Mattioli, G., Amelung, F., Jonsson, S.N., Jansma, P., Hong, S.-H., Dixon, T., Prépetit, C., Momplaisir, R., 2010. Transpressional rupture of an unmapped fault during the 2010 Haiti earthquake. Nat. Geosci. 3 (11), 794–799.
Calais, E., Camelbeeck, T., Stein, S., Liu, M., Craig, T.J., 2016. A new paradigm for large earthquakes in stable continental plate interiors. Geophys. Res. Lett. 43 (20), 10,621–10,637.
Calais, Eric, Perrot, Julie, De Lepinay, Mercier, B., 1998. Strike-slip tectonics and seismicity along the northern Caribbean plate boundary from Cuba to Hispaniola. Special Papers-Geological Society Of America 125–142.
Caputo, R., 2007. Sea-level curves: Perplexities of an end-user in morphotectonic applications. Glob. Planet. Chang. 57 (3–4), 417–423.
Clark, J.A., Farrell, W.E., Peltier, W.R., 1978. Global changes in postglacial sea level: a numerical calculation. Quat. Res. 9 (3), 265–287.
Colas, A., Sutherland, B., 2001. The World Stormrider Guide, Low Pressure.
Corbeau, J., Rolandone, F., Leroy, S., Meyer, B., Mercier de Lépinay, B., Ellouz-Zimmermann, N., Momplaisir, R., 2016. How transpressive is the northern Caribbean plate boundary? Tectonics 35 (4), 1032–1046.
Corbeau, J., Gonzalez, O.L., Clouard, V., Rolandone, F., Leroy, S., Keir, D., Stuart, G., Momplaisir, R., Boisson, D., Prépetit, C., 2019. Is the local seismicity in western Hispaniola (Haiti) capable of imaging northern Caribbean subduction? Geosphere 15 (6), 1738–1750.
Coyne, M.K., Jones, B., Ford, D.C., 2007. Highstands during marine isotope stage 5: evidence from the Ironshore formation of Gran Cayman, Brisitsh West Indies. Quat. Sci. Rev. 26, 536–559.
Crosby, W.O., 1883. Elevated coral reefs of Cuba. Ann. Mag. Nat. Hist. 12 (70), 283–284.
Cruz-Orosa, I., Sabat, F., Ramos, E., Vazquez-Taset, Y.M., 2012. Synorogenic basins of central Cuba and collision between the Caribbean and North American plates. Int. Geol. Rev. 54 (8), 876–906.
Daly, R.A., 1925. Pleistocene changes of level. Am. J. Sci. fifth serie X (58), 281–313.
Darton, N.H., 1926. Geology of the Guantanamo Basin, Cuba. J. Wash. Acad. Sci. 16 (12), 324–333.
Darwin, C.R., 1842. The Structure and Distribution of Coral Reefs. Being the First Part of the Geology of the Voyage of the Beagle, Under the Command of Capt. Fitzroy, R.N. During the Years 1832 to 1836. Smith Elder and Co, London.
Darwin, C., 1890. On the Structure and Distribution of Coral Reefs: Also Geological Observations on the Volcanic Islands and Parts of South America Visited during the Voyage of HMS Beagle, Ward, Lock.
Davis, W.M., 1915. A Shaler Memorial study of coral reefs. Am. J. Sci. (237), 223–271.
de Gelder, G., Jara-Muñoz, J., Melnick, D., Fernandez-Blanco, D., Rouby, H., Pedoja, K., Husson, L., Armijo, R., Lacassin, R., 2020. How do sea-level curves influence modeled marine terrace sequences? Quat. Sci. Rev. 229, 106–132.
De Waele, J., D'Angeli, I.M., Tisato, N., Tuccimei, P., Soligo, M., Gines, J., Gines, A., Fornos, J.J., Villa, I.M., Grau Gonzalez, E.R., Barnasconi, S.M., Bontognali, T.R.R., 2017. Coastal uplift rate at Matanzas (Cuba) inferred from MIS 5e phreatic overgrowths on speleothems. Terra Nova 29 (2), 98–105.
De Waele, J., D'Angeli, I.M., Bontognali, T., Tuccimei, P., Scholz, D., Jochum, K.P., Columbu, A., Bernasconi, S.M., Fornas, J.J., Grau Gonzalez, E.R., 2018. Speleothems in a north Cuban cave register sea-level changes and Pleistocene uplift rates. Earth Surf. Process. Landf. 43 (11), 2313–2326.
del Busto Alvarez, R., 1975. Las terrasas marinas de Maisi. In: Ciencia : Serie 7 Geografia, 10, pp. 1–12.
Diaz de Neira, J.A., Braga, J.C., Mediato, J., Lasseur, E., Monthel, J., Hernaiz, P.P., Perez-Cerdon, F., Lopera, E., Thomas, A., 2015. Plio-Pleistocene palaeogeography of the Llanura Costera del Caribe in eastern Hispaniola (Dominican Republic): interplay of geomorphic evolution and sedimentation. Sediment. Geol. 325, 90–105.
Diaz de Neira, J.A., Braga, J.C., Perez-Cerdon, F., Lopera, E., 2017. Marine terraces of the Promontorio de Cabrera (Pleistocene, northern Dominican Republic). Bol. Geol. Minero 128 (3), 657–674.
Diaz-Guanche, C., Denis-Valle, R., Ramirez-Hernandez, R., Rosa-Saavedra, C.R., Estevez-Cruz, E., Ordaz-Hernandez, A., 2014. Caracterizacion geoligica y geomorfoligica de la peninsula de Guanahacabibes, Cuba. Miner. Geol. 30 (4), 21–37.
Dodge, R.E., Fairbanks, R.G., Benninger, L.K., Maurrasse, F., 1983. Pleistocene sea levels from raised coral reefs of Haiti. Science 219 (4591), 1423–1425.
Dominguez-Gonzalez, L., Rodriguez-Infante, A., Wobbe, F., Stanek, K.P., Gloaguen, R., 2007. Morfoalineamientos en la zona costera entre el poblado de Yamanigüey y la ciudad de Baracoa. Miner. Geol. 23 (3), 17.
Ducloz, C., 1963. Etude géomorphologique de la région de Matanzas, Cuba: avec une contribution à l'étude des dépôts quaternaires de la zone Habana-Matanzas. Arch. Sci. 16 (2), 351–402.
Dumas, B., Hoang, C.T., Raffy, J., 2006. Record of MIS 5 sea-level highstands based on U/Th dated coral terraces of Haiti. In: Quaternary International Quaternary Sea-level Changes: Contributions From the 32nd IGC 145–146, pp. 106–118.
Emery, K.O., 1981. Low marine terraces of Grand Cayman Island. Estuar. Coast. Shelf Sci. 12, 569–578.
Escuder-Viruete, J., Beranoaguirre, A., Valverde-Vaquero, P., McDermott, F., 2020. Quaternary deformation and uplift of coral reef terraces produced by oblique subduction and underthrusting of the Bahama Platform below the northern Hispaniola forearc. Tectonophysics 796, 228631.
Fairbridge, R.W., 1961. Eustatic changes in sea level. Phys. Chem. Earth 4, 99–185.
Feuillet, N., Tapponnier, P., Manighetti, I., Villemant, B., King, G., 2004. Differential uplift and tilt of Pleistocene reef platforms and Quaternary slip rate on the Morne-Piton normal fault (Guadeloupe, French West Indies). J. Geophys. Res. 109 (B2), B02404.1–B02404.18.
Franco, G.F., 1983. Observaciones sobre el Neogeno-Cuaternario de la franja marina costera del extremo oriental de Cuba. Contribucion a la geologia de Cuba oriental. E. Nagy, La Havana, Editorial Cientifico-Tecnica.
Gallup, C.D., Cheng, H., Taylor, F.W., Edwards, R.L., 2002. Direct determination of the timing of sea level change during termination II. Science 295 (5553), 310–313.
Garcia, J.A., 2001. Seismic Hazard Assessment for Cuba and the Surrounding Area. Research Report. ICTP, Trieste, Italy, pp. 1–80.
Glushankova, N.I., Parunin, O.B., Timashkova, T.A., Khait, V.Z., Shlukov, A.I., 1980. Moscow MV lomonosov state university radiocarbon dates I. Radiocarbon 22 (1), 82–90.
Gordon, M.B., Mann, P., Caceres, D., Flores, R., 1997. Cenozoic tectonic history of the North America-Caribbean plate boundary zone in western Cuba. J. Geophys. Res. 102 (B5), 10055–10082.
Grant, K.M., Rohling, E.J., Ramsey, C.B., Cheng, H., Edwards, R.L., Florindo, F., Heslop, D., Marra, F., Roberts, A.P., Tamisiea, M.E., 2014. Sea-level variability over five glacial cycles. Nat. Commun. 5 (5076).
Guilcher, A., 1969. Pleistocene and Holocene Sea level changes. Earth Sci. Rev. 5, 69–97.
Gutiérrez-Domech, R., Duarte-Barrientos, A., 2001. Las unidades litoestratigraficas carsificadas de Cuba Occidenta. IV Congreso de Geologia y Mineria : Geologia del Cuaternario, geomorfologia y carso, La Habane. GQGC, pp. 1–75.
Hastie, A.R., Mitchell, S.F., Treloar, P.J., Kerr, A.C., Neill, I., Barfod, D.N., 2013. Geochemical components in a cretaceous island arc: the Th/La-(Ce/Ce*) Nd diagram and implications for subduction initiation in the inter-American region. Lithos 162, 57–69.
Hearty, P.J., Neumann, A.C., O'Leary, M.J., 2007. Comment on "Record of MIS 5 sea-level highstands based on U/Th dated coral terraces of Haiti" by Dumas et al. [Quaternary International 2006 106-118]. Quat. Int. Soil Rec. Quat. Clim. Change 162-163, 205–208.
Hibbert, F.D., Rohling, E.J., Dutton, A., Williams, F.H., Chutcharavan, P.M., Zhao, C., Tamisiea, M.E., 2016. Coral indicators of past sea-level change: a global repository of U-series dated benchmarks. Quat. Sci. Rev. 145, 1–56.
Hill, R.T., 1894. Notes on the Tertiary and later history of the Island of Cuba. Am. J. Sci. 3 (285), 196–212.
Hill, R.T., 1895. Notes on the Geology of the Island of Cuba: Based Upon a Reconnoissance Made for Alexander Agassiz, Museum.
Hippolyte, J.-C., Mann, P., 2011. Neogene–Quaternary tectonic evolution of the Leeward Antilles islands (Aruba, Bonaire, Curaçao) from fault kinematic analysis. Mar. Pet. Geol. 28, 259–277.
Horsfield, W.T., 1975. Quaternary vertical movements in the greater Antilles. Geol. Soc. Am. Bull. 86, 933–938.
Husson, L., Pastier, A.-M., Pedoja, K., Elliot, M., Paillard, D., Authemayou, C., Sarr, A.-C., Schmitt, A., Cahyarini, S.Y., 2018. Reef carbonate productivity during Quaternary sea level oscillations. Geochem. Geophys. Geosyst. 19 (4), 1148–1164.

Iturralde-Vinent, M., 1967. Estudio Geologico Preliminar del Municipio de Manguito, Provincia de Matanzas, Cuba, 4. Instituto Nacional de Recursos Hidraulicos, Publ. Esp., pp. 11–22
Iturralde-Vinent, M., 1969a. El Neogeno en la provincia de Matanzas, Cuba. In: Parte General. Publicacion Especial del Instituto Nacional de Recursos Hidraulicos, 7, pp. 3–30.
Iturralde-Vinent, M.A., 1969b. Principal characteristics of Cuban Neogene stratigraphy. AAPG Bull. 53 (9), 1938–1955.
Iturralde-Vinent, M.A., 1977. Los movimientos tectonicos de la etapa de desarrollo plataformico en Cuba. In: Informes Cientifico-Tecnicos Academia de Ciencas de Cuba, 20, pp. 3–24.
Iturralde-Vinent, M.A., 1981. Nuevo modelo interpretativo de la evolucion geologica de Cuba.
Iturralde-Vinent, M.A., 1982. Aspectos geologicos de la biogeografia de Cuba. Rev. Cien. de Tierra Espacio 5, 85–100.
Iturralde-Vinent, M.A., 1994. Cuban geology: a new plate-tectonic synthesis. J. Pet. Geol. 17 (1), 39–69.
Iturralde-Vinent, M.A., 1996. Cuba: el arco de islas volcanicas del Cretacico. In: Ofiolitas y arcos volcanicos de Cuba. IGCP project, 364, pp. 179–189.
Iturralde-Vinent, M.A., 2003. Ensayo sobre la paleogeografia del Cuaternario de Cuba. V Congreso de Geologia y Mineria, La Habana.
Iturralde-Vinent, M., 2013. Tipologia y evolucion de las zonas costeras de Cuba. V convencion Cubana de Ciencias de la Tierra, La Havana.
James, N.P., Mountjoy, E.W., Omura, A., 1971. An early Wisconsin reef terrace at Barbados, West Indies, and its climatic implications. Geol. Soc. Am. Bull. 82 (7), 2011–2017.
Jara-Muñoz, J., Melnick, D., Pedoja, K., Strecker, M.R., 2019. TerraceM-2: a Matlab® interface for mapping and modeling marine and lacustrine terraces. Front. Earth Sci. 7, 255.
Jennings, O.E., 1913. Note on the geology of the Isle of Pines, Cuba. J. Geol. 21 (4), 367–369.
Johnson, R.G., 2001. Last interglacial sea stands on Barbados and an early anomalous deglaciation timed by differential uplift. J. Geophys. Res. 106 (C6), 11 543–11 551.
Johnson, M.E., Libbey, L.K., 1997. Global review of upper Pleistocene (substage 5e) rocky shores: tectonic segregation, substrate variation, and biological diversity. J. Coast. Res. 13 (2), 297–307.
Jones, W.F., 1918. A Geological Reconnaissance in Haiti a Contribution to Antillean Geology. J. Geol. 26 (8), 728–752.
Kartashov, I.P., Mayo, N.A., 1974. Principales rasgos del desarrollo geologico de Cuba Oriental en el Cenozoico tardio. In: Contribucion a la Geologia de Cuba, Publicacion Especial, 2, pp. 165–174.
Kartashov, I.P., Mayo, N., 1976. Descripcion de algunas formaciones geologicas del sistema Cuaternario de Cuba, reconocidas recientemente. Acad. Cien. Cuba 26, 1–12.
Kartashov, I.P., Cherniajovski, A., Peñalver, L.L., 1981. El Antropogeno de Cuba. Edit. Nauka. Moscu 356, 1–145.
Khan, N.S., Ashe, E., Horton, B.P., Dutton, A., Kopp, R.E., Brocard, G., Engelhart, S.E., Hill, D.F., Peltier, W.R., Vane, C.H., 2017. Drivers of Holocene sea-level change in the Caribbean. Quat. Sci. Rev. 155, 13–36.
Lajoie, K.R., 1986. Coastal Tectonics. Active Tectonic. N. A. Press. National Academic Press, Washington D.C, pp. 95–124.
Leroy, S., Mauffret, A., Patriat, P., Mercier de Lépinay, B., 2000. An alternative interpretation of the Cayman trough evolution from a reidentification of magnetic anomalies. Geophys. J. Int. 141 (3), 539–557.
Leroy, S., Ellouz-Zimmermann, N., Corbeau, J., Rolandone, F., de Lepinay, B.M., Meyer, B., Momplaisir, R., Granja Bruja, J.L., Battani, A., Baurion, C., 2015. Segmentation and kinematics of the North American-Caribbean plate boundary offshore Hispaniola. Terra Nova 27 (6), 467–478.
Léticée, J.-L., Cornée, J.-J., Münch, P., Fietzke, J., Philippon, M., Lebrun, J.-F., De Min, L., Randrianasolo, A., 2019. Decreasing uplift rates and Pleistocene marine terraces settlement in the central lesser Antilles fore-arc (La DÃ©sirade Island, 16Â° N). Quat. Int. 508, 43–59.
Lisiecki, L.E., Raymo, M.E., 2005. A Pliocene-Pleistocene stack of 57 globally distributed benthic delta 18 O records. Paleoceanography 20, PA1003.
Lyell, C., 1830. Principles of Geology, Being an Attempt to Explain the Former Changes of the Earth's Surface, by Reference to Causes Now in Operation. John Murray, London.
Mann, P., Burke, K., 1984. Neotectonics of the Caribbean. Rev. Geophys. 22 (4), 309–362.
Mann, P., Schubert, C., Burke, K., 1990. Review of Caribbean neotectonics. In: gna 1990, pp. 307–338.
Mann, P., Tyburski, S.A., Rosencrantz, E., 1991. Neogene development of the Swan Islands restraining-bend complex, Caribbean Sea. Geology 19 (8), 823–826.
Mann, P., Taylor, F.W., Edwards, R.L., Ku, T.-L., 1995. Actively evolving microplate formation by oblique collision and sideways motion along strike-slip faults: an example from the northeastern Caribbean plate margin. Tectonophysics 246 (1–3), 1–69.
Mann, P., Hippolyte, J.-C., Grindlay, N.R., Abrams, L.J., 2005. Neotectonics of southern Puerto Rico and its offshore margin. In: Active Tectonics and Seismic Hazards of Puerto Rico, the Virgin Islands, and Offshore Areas, 385, pp. 173–214.
Marie-Victorin, F., Léon, F., 1956. Itinéraires botaniques dans l'ile de Cuba. Institut botanique de l'Université de Montréal, Montréal, Canada.
Massip, S., 1936. Estructura y relieve de Cuba. In: Bol. Soc. Geol. Mexicana, IX(4), pp. 177–196.
Matley, C.A., 1926. The geology of the Cayman Islands (British West Indies), and their relation to the Bartlett Trough. Q. J. Geol. Soc. 82 (1–4), 352–387.
Meinzer, O.E., 1933. Geologic reconnaissance of a region adjacent to Guantanamo Bay, Cuba. J. Wash. Acad. Sci. 23 (5), 246–263.
Mesolella, K.J., 1967. Zonation of uplifted Pleistocene coral reefs on Barbados, West Indies. Science 156 (3775), 638–640.
Mesolella, K.J., Matthews, R.K., Broecker, W.S., Thurber, D.L., 1969. The astronomical theory of climatic change: barbados data. J. Geol. 77 (3), 250–274.
Mitchell, S.F., Pickerill, R.K., Blackwell, B.A.B., Skinner, A.R., 2000. The age of the Port Morant formation, south-eastern Jamaica. Carribean J. Earth Sci. 34, 1–4.
Mitchell, S.F., Pickerill, R.K., Stemann, T.A., 2001. The Port Morant Formation (Upper Pleistocene, Jamaica): high resolution sedimentology and paleoenvironmental analysis of a mixed carbonate clastic lagoonal succession. Sediment. Geol. 144 (3–4), 291–306.
Molerio-Leon, L.F., 2005. Los nichos de marea karsticos en Cuba y las fluctuaciones del nivel del mar en el cuaternario. Bol. Soc. Venezolana Espeleol. 39, 16–20.
Molerio-Léon, L.F., 2017a. Neotectonica y patrones de cavernamiento en Punta Guanos, Matanzas, Cuba I: el entorno geologico. Gota Gota 14, 11–20.
Molerio-Léon, L.F., 2017b. Neotectonica y patrones de cavernamiento en Punta Guanos, Matanzas, Cuba III. El desarrollo del Karzt. Gota Gota 14, 11–20.
Montaggioni, L., Braithwaite, C.J.R., 2009. Quaternary Coral Reef Systems : History, Development Processes and Controlling Factors. Elsevier, Amsterdam.
Muhs, D.R., 2001. Evolution of soils on quaternary reef terraces of Barbados, West Indies. Quat. Res. 56 (1), 66–78.
Muhs, D.R., Schweig, E.S., Simmons, K.R., Halley, R.B., 2018. Late Quaternary uplift along the North America-Caribbean plate boundary: evidence from the sea level record of Guantanamo Bay, Cuba. Quat. Sci. Rev. 178, 54–76.
Murray-Wallace, C., Woodroffe, C., 2014. Quaternary Sea Level : A Global Perspective. Cambridge University Press, Cambridge.
Naprstek, V., 1978. Radiometric age and genesis of the Jaimanitas formation in the Rincon de Guanabo region, Cuba. Vestnik Ustredniho Ustavu Geologickeho 53 (1), 19–28.
Nuñez, K., 2001. La inluencia de la falla Oriente en la estructura geologica del area de San Antonio del Sur, Cuba. IV Congreso de Geologia y Mineria ; Geologia Regional, La Habana. Memorias GEOMIN, pp. 67–75.
Pajon, J.M., Hernendez, I., Estevez, Y., 2006. Paleoregistros de las variaciones del nivel del mar en el Caribe durante el Pleistoceno-Holoceno. Conexion con problemas de la Arqueologia cubana. In: Memorias de la VIII Conferencia Internacional Antropologia 2006 La Antropologia ante los Nuevos Retos de la Humanidad, La Havana.
Pastier, A.M., Husson, L., Pedoja, K., Bézos, A., Authemayou, C., AriasRuiz, C., Cahyarini, S.Y., 2019. Genesis and architecture of sequences of quaternary coral reef terraces: insights from numerical models. Geochem. Geophys. Geosyst. 20 (8), 4248–4272.
Pedoja, K., Husson, L., Regard, V., Cobbold, P.R., Ostanciaux, E., Johnson, M.E., Kershaw, S., Saillard, M., Martinod, J., Furgerot, L., Weill, P., Delcaillau, B., 2011. Relative sea-level fall since the last interglacial stage: are coasts uplifting worldwide? Earth Sci. Rev. 108 (1–2), 1–15.
Pedoja, K., Husson, L., Johnson, M.E., Melnick, D., Witt, C., Pochat, S., Nexer, M., Delcaillau, B., Pinegina, T., Poprawski, Y., Authemayou, C., Elliot, M., Regard, V., Garestier, F., 2014. Coastal staircase sequences reflecting sea-level oscillations and tectonic uplift during the Quaternary and Neogene. Earth Sci. Rev. 132, 13–38.
Pedoja, K., Husson, L., Bezos, A., Pastier, A.-M., Imran, A.M., Arias-Ruiz, C., Sarr, A.-C., Elliot, M., Pons-Branchu, E., Nexer, M.L., 2018. On the long-lasting sequences of coral reef terraces from SE Sulawesi (Indonesia): distribution, formation, and global significance. Quat. Sci. Rev. 188, 37–57.
Peñalver, L.L., 1982. Correlacion estratigrafica entre los depositos cuaternarios de la plataforma noroccidental de Pinar del Rio y las zonas emergidas proximas. Rev. Cien. Tierra Espacio 5, 63–84.
Peñalver, L.L., Barrientos Duarte, A., Oro Alfonso, J.R., 1982a. Las secuencias terrigenas del Plioceno Superior-Pleistoceno" humedo" de Cuba occidental. Rev. Cien. Tierra Espacio 5 (43–62).
Peñalver, L.L., Oro Alfonso, J.R., Barrientos Duarte, A., 1982b. Las secuencias carbonatadas del Plioceno-Pleistoceno" humedo" de Cuba occidental. Rev. Cien. Tierra Espacio 5 (24–42).
Peñalver, L.L., Lavandero, R., Barriendo, A., 1997. Sistema cuaternario. Estudios sobre Geologia de Cuba. G. Furrazola-Bermudez and Nunez-Cambra. Instituto de Geologia y Paleontologia, La Havana, pp. 165–178.
Peñalver, L.L., Barrientos, A., Orbera, L., Hernandez, C., Estrada, V., Napoles, E., Alvarez, J., Perez Laso, J., Mendez, A., Fundora, M., 1998. Version actualizada del mapa de depositos Cuaternarios de Cuba y su plataforma insular a escala 1: 500 000. Geol. Miner. 98, 559–561. Memorias, Tomo 1. 1.
Peñalver, L.L., Cabrera, M., Trujillo, H., Morales, M., Fundora, M., Perez Lazo, J., Guerra, M., Pedroso, I., 2001. Evolucion paleoclimatica y paleogeografica de Cuba durante el Cuaternario. IV Congreso de Geologia y Mineria, La Habana.
Peñalver, L.L., Castellanos, E., Perez, R., Rivada, R., 2003. Las terrazas marinas de Cuba y su correlacon con algunas del area circumcaribe. In: Geologia del Cuaternario, geomorfologÃa y carso. La Habana, Memorias Geominerales, pp. 1–10.
Perera, Y., Rojas, C., 2005. Distribucion facial de los corales de la formacion Jaimanitas en una area al oeste de Cojimar, ciudad de la Habana. In: VI congreso de Geolgia (Geologia 2005): Geologia del Cuaternario y Carsologia, La Habana, Geosciencas.
Pérez, C.M., Castellanos, E., Peñalver, L., Cabrera, M., Denis, R., 2008. Aplicaciones de la teledeteccion al estudio de los depositos cuaternarios cubanos. XIII Simposio internacional de la sociedad latinoamericana de percepcion remota y sistemas de informacion espacial 1–11.
Pérez Lazo, J., 1986. Escala paleomagnética condicional para los depositos del intervalo Plioceno-Cuaternario de Cuba. ISPJAE, La Habana.
Pérez, C.M., Peñalver, L.L., Cabrera, M., Denis, R., 2003. Algunas consideraciones acerca de la evolucion tectonica del extremo occidental de Pinar del Rio, Cuba. In:

Memorias del V Congreso Internacional de Geologia y Mineria. CD GEOMIN-2003, La Habana.
Pérez, C., Peñalver, L., Rivada, R., 2011. San Antonio del Sur : Paleobahia de bolsa durante el Pleistoceno Superior. In: IX congreso Cubano de Geologia: Geologia regional y Tectonica, La Habana.
Perez-Aragon, R.O., Peñalver, L., Triff-Oquendo, J., Rivada-Suaez, R., 2001. Nuevos datos sobre la geomorfologia de las terrazas marinas de la region Habana-Matanzas. IV Congreso de Geologia y Mineria La Havana.
Perrot, J., Calais, E., De Lepinay, B.M., 1997. Tectonic and kinematic regime along the Northern Caribbean Plate Boundary: new insights from broad-band modeling of the May 25, 1992, Ms= 6.9 Cabo Cruz, Cuba, earthquake. Pure Appl. Geophys. 149 (3), 475–487.
Pindell, J., Kennan, L., Maresch, W.V., Stanek, K., Draper, G., Higgs, R., 2005. Plate-kinematics and crustal dynamics of circum-Caribbean arc-continent interactions: tectonic controls on basin development in Proto-Caribbean margins. Spec. Pap. Geol. Soc. Am. 394, 7.
Pindell, J., Maresch, W.V., Martens, U., Stanek, K., 2012. The Greater Antillean Arc: Early Cretaceous origin and proposed relationship to Central American subduction mélanges: implications for models of Caribbean evolution. Int. Geol. Rev. 54 (2), 131–143.
Possee, D., Keir, D., Harmon, N., Rychert, C., Rolandone, F., Leroy, S., Corbeau, J., Stuart, G., Calais, E., Illsley-Kemp, F., 2018. The tectonics and active faulting of Haiti from seismicity and tomography. Tectonics 38 (3), 1138–1155.
Potter, E.-K., Esat, T.M., Schellmann, G., Radtke, U., Lambeck, K., McCulloch, M.T., 2004. Suborbital-period sea-level oscillations during marine isotope substages 5a and 5c. Earth Planet. Sci. Lett. 225 (1–2), 191–204.
Prentice, C.S., Mann, P., Crone, A.J., Gold, R.D., Hudnut, K.W., Briggs, R.W., Koehler, R. D., Jean, P., 2010. Seismic hazard of the Enriquillo-Plantain Garden fault in Haiti inferred from palaeoseismology. Nat. Geosci. 3 (11), 789–793.
Pubellier, M., Mauffret, A., Leroy, S., Vila, J.M., Amilcar, H., 2000. Plate boundary readjustment in oblique convergence: example of the Neogene of Hispaniola, Greater Antilles. Tectonics 19 (4), 630–648.
Pushcharovski, Y., 1988. Mapa geologico de la Republica de Cuba, escala 1: 250,000. Academies of Sciences of Cuba and the USSR, Ciudad de La Habana and Moscow.
Radtke, U., Schellmann, G., 2006. Uplift history along the Clermont Nose Traverse on the west coast of Barbados during the last 500,000 years - implications for paleo-sea level reconstructions. J. Coast. Res. 22 (2), 350–356.
Richards, H.G., 1935. Pleistocene mollusks from western Cuba. J. Paleontol. 253–258.
Rodriguez-Cotilla, M.O., 2014. Alternative interpretation for the active zones of Cuba. Geotectonics 48 (6), 459–482.
Rohling, E.J., Grant, K., Bolshaw, M., Roberts, A.P., Siddall, M., Hemleben, C., Kucera, M., 2009. Antarctic temperature and global sea level closely coupled over the past five glacial cycles. Nat. Geosci. 2, 500–504.
Rojas, R., Abreu, E., Diaz-Guanche, C., Pajon, J., 2017. Paleovientos intensos del Este-Noreste durante el Pleistoceno temprano memorizados en las eolianitas de la formacion Guanabo, La Habana, Cuba occidental. In: XII Congreso de Geologia : Estratigrafia y Paleontologia, La Habana.
Rojas-Agramonte, Y., Neubauer, F., Handler, R., Garcia-Delgado, D.E., Friedl, G., Delgado-Damas, R., 2005. Variation of palaeostress patterns along the Oriente transform wrench corridor, Cuba: significance for Neogene-Quaternary tectonics of the Caribbean realm. Tectonophysics 396 (3–4), 161–180.
Rovere, A., Raymo, M.E., Vacchi, M., Lorscheid, T., Stocchi, P., Gomez-Pujol, L., Harris, D.L., Casella, E., O'Leary, M.J., Hearty, P.J., 2016. The analysis of Last Interglacial (MIS 5e) relative sea-level indicators: reconstructing sea-level in a warmer world. Earth Sci. Rev. 159, 404–427.
Rubio-Sandoval, K., Rovere, A., Cerrone, C., Stocchi, P., Lorscheid, T., Felis, T., Petersen, A.-K., Ryan, D.D., 2021. A review of Last Interglacial sea-level proxies in the Western Atlantic and Southwestern Caribbean, from Brazil to Honduras. Earth Syst. Sci. Data Discuss. 1–41.
Salomon, J.-N., 1995. Relations entre karsts, aquifères et niveaux de la mer à Cuba. Hommes et terres du Nord 1 (1), 82–96.
Schellmann, G., Radtke, U., 2004. A revised morpho- and chronostratigraphy of the Late and Middle Pleistocene coral reef terraces on Southern Barbados (West Indies). Earth Sci. Rev. 64 (3–4), 157–187.
Schellmann, G., Radtke, U., Potter, E.-K., Esat, T.M., McCulloch, M.T., 2004. Comparison of ESR and TIMS U/Th dating of marine isotope stage (MIS) 5e, 5c, and 5a coral from Barbados–implications for palaeo sea-level changes in the Caribbean. In: Quaternary International Coastal Environmental Change during Sea-Level Highstands, IGCP 437 Symposium, Barbados, 120(1), pp. 41–50.
Schielein, P., Burow, C., Pajon, J., Consuegra, R.R., Zhao, J.-x., Schellmann, G., 2020. ESR and U-Th dating results for Last Interglacial coral reef terraces at the northern coast of Cuba. Quat. Int. 256, 216–229.
Shackleton, N.J., 1987. Oxygen Isotopes, Ice volume and Sea Level. Quat. Sci. Rev. 6, 183–190.
Shakun, J.D., Lea, D.W., Lisiecki, L.E., Raymo, M.E., 2015. An 800-kyr record of global surface ocean Î18O and implications for ice volume-temperature coupling. Earth Planet. Sci. Lett. 426, 58–68.
Shantzer, E.V., Petrov, O.M., Franco, G.F., 1976. Sobre las terrazas marinas costeras y los depesitos relacionados con ellas (en ruso).Acumulacion de sedimentos cuaternarios y formacion del relieve (Edit. Nauka, Moscow), pp. 34–80.
Shanzer, E.V., Petrov, O.M., Franco, G.L., 1975. Sobre las informaciones costeras del Holoceno en Cuba. Las terrazas pleistocénicas de la Región Habana-Matanzas y los sedimentos vinculados a ellas. Academia de Ciencias de Cuba, 21. serie Geologia, pp. 3–26.
Siddal, M., Chappell, J., Potter, E.-K., 2006. Eustatic sea level during past interglacials. In: Sirocko, F., Claussen, M., Goñi, M.F. Sanchez, Litt, T. (Eds.), The Climate of Past Interglacials. Elsevier, Amsterdam, pp. 75–92.
Simms, A.R., 2021. Last interglacial sea levels within the Gulf of Mexico and northwestern Caribbean Sea. Earth Syst. Sci. Data 13 (3), 1419–1439.
Speed, R.C., Cheng, H., 2004. Evolution of marine terraces and sea level in the last interglacial, Cave Hill, Barbados. Geol. Soc. Am. Bull. 116 (1–2), 219–232.
Spencer, J.W., 1895. Geographical evolution of Cuba. Bull. Geol. Soc. Am. 7 (1), 67–95.
Spencer, T., 1985. Marine erosion rates and coastal morphology of reef limestones on Grand Cayman Island, West Indies. Coral Reefs 4 (2), 59–70.
Spratt, R.M., Lisiecki, L.E., 2016. A Late Pleistocene sea level stack. Clim. Past 12 (4), 1079.
Stirling, C.H., Esat, T.M., Lambeck, K., McCulloch, M.T., 1998. Timing and duration of the Last Interglacial: evidence for a restricted interval of widespread coral reef growth. Earth Planet. Sci. Lett. 160 (3–4), 745–762.
Symithe, S., Calais, E., De Chabalier, J.B., Robertson, R., Higgins, M., 2005. Current block motions and strain accumulation on active faults in the Caribbean. J. Geophys. Res. 120 (5), 3748–3774.
Szabo, B.J., 1979. 230Th, 231Pa, and open system dating of fossil corals and shells. J. Geophys. Res. 84 (C8), 4927–4930.
Taber, S., 1922. The great fault troughs of the Antilles. J. Geol. 30 (2), 89–114.
Taber, S., 1931. The structure of the Sierra Maestra near Santiago de Cuba. J. Geol. 39 (6), 532–557.
Thompson, W.G., Spiegelman, M.W., Goldstein, S.L., Speed, R.C., 2003. An open-system model for U-series age determinations of fossil corals. Earth Planet. Sci. Lett. 210 (1–2), 365–381.
Toscano, M.A., Rodriguez, E., Lundberg, J., 1999. Geologic investigation of the late Pleistocene Jaimanitas Formation: science and society in Castro's Cuba. In: Proceedings of the 9th Symposium on the Geology of the Bahamas and Other Carbonate Regions, San Salvador, Bahamas, Bahamian Field Station.
Trechmann, C.T., 1933. The uplift of Barbados. Geol. Mag. 70 (1), 19–47.
Vaughan, T.W., 1914. Sketch of the geologic history of the Florida coral reef tract and comparisons with other coral reef areas. J. Wash. Acad. Sci. 4 (2), 26–34.
Vaughan, T.W., Spencer, A.C., 1902. The geography of Cuba. Bull. Am. Geogr. Soc. 34 (2), 105–116.
Villemant, B., Feuillet, N., 2003. Dating open systems by the 238U-234U-230Th method: application to Quaternary reef terraces. Earth Planet. Sci. Lett. 210 (1–2), 105–118.
Waelbroeck, C., Labeyrie, L.D., Michel, E., Duplessy, J.C., McManus, J.F., Lambeck, K., Balbon, E., Labracherie, M., 2002. Sea-level and deep water temperature changes derived from benthic foraminefera isotopic records. Quat. Sci. Rev. 21, 295–305.
Wessels, R.J.F., Ellouz-Zimmermann, N., Bellahsen, N., Hamon, Y., Rosenberg, C., Deschamps, R., Momplaisir, R., Boisson, D., Leroy, S., 2019. Polyphase tectonic history of the Southern Peninsula, Haiti: from folding-and-thrusting to transpressive strike-slip. Tectonophysics 751, 125–149.
Woodring, W.P., 1954. Caribbean land and sea through the ages. Geol. Soc. Am. Bull. 65 (8), 719–732.
Woodroffe, C.D., Stoddart, D.R., Harmon, R.S., Spencer, T., 1983. Coastal morphology and late quaternary history, Cayman Islands, West Indies. Quat. Res. 19 (1), 64–84.
Yildirim, C., Melnick, D., Ballato, P., Schildgen, T.F., Echtler, H., Erginal, A.E., Kayak, N., Strecker, M.R., 2013. Differential uplift along the northern margin of the Central Anatolian Plateau: inferences from marine terraces. Quat. Sci. Rev. 81, 12–28.
Zachos, J.C., Dickens, G.R., Zeebe, R.E., 2008. An early Cenozoic perspective on greenhouse warming and carbon-cycle dynamics. Nature 451 (7176), 279–283.
Zenkovichy, V.P., Ionin, A.S., 1969. Breve resumen sobre las investigaciones de la estructura y dinamica de la zona litoral de la Isla de Cuba. Serie Oceanologica 8, 1–22.